Supporting Information

Well-Organized Columnar Superlattices via Positive Coupling between Polymer Backbone and Discotic Side-Groups

Bin Mu,[†] Shi Pan,[†] Huafeng Bian,[†] Bin Wu,[†] Jianglin Fang,[‡] and Dongzhong Chen*[,†]

[†]*Key Laboratory of High Performance Polymer Materials and Technology of Ministry of Education, Collaborative Innovation Center of Chemistry for Life Sciences, Department of Polymer Science and Engineering, School of Chemistry and Chemical Engineering, Nanjing University, Nanjing 210093, China.*
[‡]*Center for Materials Analysis, Nanjing University, Nanjing 210093, China*

*Corresponding author, Email: cdz@nju.edu.cn, Phone: +86-25-83686621, Fax: +86-25-83317761.

Table of Contents

1. Materials and Measurements

Materials

The synthesis of 2-hydroxy-3,6,7,10,11-penta(hexyloxy)triphenylene (**1**) and chain transfer agent (CTA) of 2-(methyl propionate)-(*O*-ethyl xanthate) was conducted according to the same procedure as described in our previous reports.[1,2] Acryloyl chloride (>95%, TCI), acrylic acid (99%), Chloromethyl chlorosulfate (96%), tetrabutylammonium hydrogensulfate (98%), sodium hydride (>95%, moistureproofed with oil), tetrabutylammonium bromide (99%), 1,2-dibromoethane (99%, Acros), 1,3-dibromopropane (>98%, TCI), 1,4-dibromobutane (99%, Alfa-Aesar), 1,5-dibromopentane (>98%, TCI), 1,6-dibromohexane (96%, Sigma-Aldrich), 1,7-dibromoheptane (>98%, TCI), 1,8-dibromooctane (98%, Alfa-Aesar), 1,9-dibromononane (>95%, TCI), 1,10-dibromodecane (97%, Sigma-Aldrich), Tetradecanedioic acid (98%), lithium aluminum hydride solution in THF (1.0 M, Sigma-Aldrich), triphenylphosphine (99%), N-bromosuccinamide (99%) was used as received. Triethylamine (99%) was refluxed over calcium hydride and freshly redistilled before use. Dichloromethane (DCM) was refluxed over calcium hydride and distilled before use. Tetrahydrofuran (THF) and 1,4-dioxane were refluxed over sodium/benzophenone until the solution turned purple and distilled before use. The 2,2-azobis(isobutyronitrile) (AIBN, 99%) was recrystallized twice from ethanol and dried under vacuum at room temperature. All other chemical reagents were commercially available and used as received.

Measurements

^{1}H NMR spectra in solution were obtained from 300 MHz (Bruker DRX 300) and 500 MHz (Bruker DRX 500) instruments. Fourier transform infrared spectra (FT-IR) were recorded on a NICOLET iS10 infrared spectrometer. Mass spectra was recorded on a LCMS-2020 single quadrupole equipped with an electrospray ionization (ESI) source interface (Shimadzu). Elemental analyses (EA) were carried out with an Elementar Vario MICRO (Germany). Gel-permeation chromatography (GPC) measurements were performed at 25 °C on a Waters 515 equipped with Wyatt Technology Optilab rEX differential refractive index and UV detectors. THF was used as the eluent at a flow rate of 1.0 mL min^{-1}, the solvent THF and sample solutions were filtered over filters with pore size of 0.45 μm (Nylon, Millex-HN 13 mm Syringes

Filters, Millipore, US). Relative weight average (M_w) and number average (M_n) molecular weights were calculated with a calibration curve based on a group of polystyrene standard samples.

Differential scanning calorimetry (DSC) thermograms were recorded on a Perkin-Elmer Pyris I calorimeter equipped with a cooling accessory and under an argon atmosphere. Typically, about 8 mg of the solid sample was encapsulated in a sealed aluminum pan with an identical empty pan as the reference. Indium was used as a calibration standard. The polarized optical microscopy (POM) was adopted to characterize thermal transitions, observe and photograph textures with a PM6000 microscope under cross-polarizers equipped with a Leitz-350 heating stage and an associated Nikon (D3100) digital camera. The samples were prepared by melt-pressing and sandwiched between two glass plates. X-ray scattering experiments were performed with a high-flux small-angle X-ray scattering instrument (SAXSess mc^2, Anton Paar) equipped with Kratky block-collimation system and a temperature control unit (Anton Paar TCS 120 and TCS 300). Both small angle X-ray scattering (SAXS) and wide angle X-ray scattering (WAXS) were simultaneously recorded on an imaging-plate (IP) which extended to high-angle range (the q range covered by the IP was from 0.06 to 29 nm^{-1}, $q = 4\pi\sin\theta/\lambda$, where the wavelength λ is 0.1542 nm of Cu-Kα radiation and 2θ is the scattering angle) at 40 kV and 50 mA. The powder samples were encapsulated with aluminum foil during the measurement and the obtained X-ray analysis data were processed with the associated SAXSquant software 3.80 and the aluminum foil background signal was subtracted.

2. Synthesis of Discotic Mesogenic TP-Acrylate Monomers

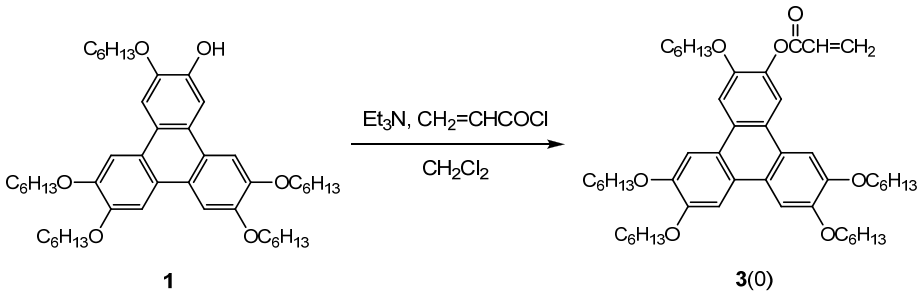

1 **3**(0)

Scheme S1. Synthesis of TP-acrylate monomer **3**(0)

3,6,7,10,11-pentakis(hexyloxy)triphenylene-2-yl acrylate (**3**(0))**.** A mixed solution of **1** (3.5 g, 4.70 mmol) and triethylamine (1.0 mL, 7.16 mmol) in DCM (70 mL) was prepared, under a nitrogen atmosphere in ice-water bath, and then a solution of acryloyl chloride (0.57 mL, 7.02 mmol) in 35 mL DCM was added slowly by using a pressure-equalizing dropping funnel over 1.5 h. The mixture was stirred for another 0.5 h, washed twice with water, and dried over anhydrous magnesium sulfate. After removal of solvent, the crude product was purified by silica-gel column chromatography using mixed solvents of petroleum ether / ethyl acetate (40 : 1, v/v) as the eluent. After dried at 35 °C under vacuum overnight to obtain 3.4 g monomer **3**(0) in yellow solid (yield 90%). ^{1}H NMR (300 MHz, $CDCl_3$) δ (ppm): 8.13 (s, 1H, Ar-H *ortho* to OCO), 7.83 (m, 5H, other Ar-H), 6.71, 6.47, 6.09 (m, 3H, C*H*$_2$C*H*CO), 4.24 (m, 10H, OCH_2), 2.02-1.89 (m, 10H, OCH_2CH_2), 1.65-1.51 (m, 10H, $O(CH_2)_2CH_2$), 1.47-1.31 (m, 20H, $O(CH_2)_3(CH_2)_2$), 0.94 (t, 15H, J = 6.7 Hz, CH_3CH_2). ESI-MS (*m/z*): $[M + Na]^+$ calcd for $C_{51}H_{74}NaO_7$, 821.53; found, 821.70.

The synthesis of (3,6,7,10,11-pentakis(hexyloxy)triphenylene-2-yloxy)methyl acrylate (**3**(1)) was conducted referring to the literature approach.[3]

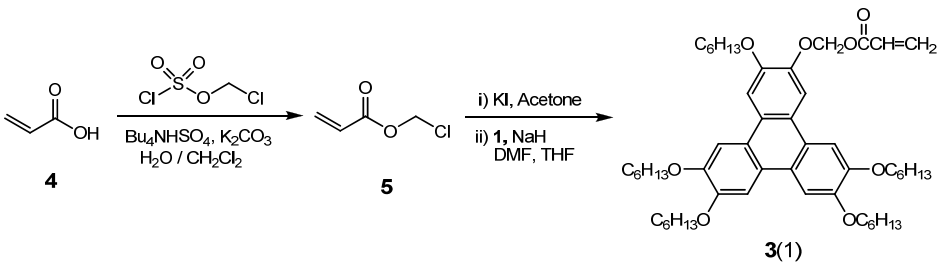

Scheme S2. Synthesis of TP-acrylate monomer **3**(1)

Chloromethyl acrylate (5). A mixed solution of tetrabutylammonium hydrogensulfate (0.47 g, 1.38 mmol) and potassium carbonate (7.67 g, 91.31 mmol) in 17 mL water and 17 mL DCM was prepared under a nitrogen atmosphere, then acrylic acid **4** (1.0 g, 13.89 mmol) and a solution of chloromethyl chlorosulfate (2.75 g, 16.67 mmol) in 8 mL DCM was added. The mixture was stirred at room temperature for 3 h, diluted with 30 mL water and 50 mL DCM, after separation of the aqueous layer was further extracted with 2 × 50 mL DCM, then all the organic layers were combined and dried over anhydrous

magnesium sulfate, filtered and concentrated under reduced pressure. The obtained pale yellow liquid was purified by silica-gel column chromatography with DCM as the eluent, after concentrated 1.05 g **5** in colorless liquid was obtained (yield 63%). ^{1}H NMR (300 MHz, $CDCl_3$) δ (ppm): 6.56, 6.18, 6.00 (m, 3H, C*H*$_2$C*H*CO), 5.81 (s, 2H, CH_2Cl). ^{13}C NMR (75 MHz, $CDCl_3$) δ (ppm): 164.2, 133.6, 127.3, 69.0.

(3,6,7,10,11-pentakis(hexyloxy)triphenylene-2-yloxy)methyl acrylate (**3**(1))**.** A mixture of **5** (1.05 g, 8.71 mmol) and KI (5.6 g, 33.7 mmol) in 40 mL acetone was stirred at room temperature for 24 h, and filtrated to remove the white precipitate. After removal of the solvent, the residue was applied to silica-gel column chromatography with DCM as the eluent, after concentrated under reduced pressure to obtain iodomethyl acrylate in colourless liquid.

A solution of **1** (3.0 g, 4.0 mmol) in 30 mL DMF was treated with NaH (0.15 g, 5.9 mmol). After reaction 30 min at room temperature, the reaction mixture was cooled to −60 °C, and a solution of iodomethyl acrylate (0.85 g, 4.0 mmol) in 5 mL THF was added. The mixture was stirred for another 1.0 h, and then raised to room temperature continued the reaction for 2 h. The resulting mixture was poured into 50 mL water and extracted with DCM, the organic layers were combined and dried over anhydrous magnesium sulfate. After removal of the solvent, the crude product was purified by silica-gel column chromatography using mixed solvents of petroleum ether / ethyl acetate (40 : 1, v/v) as the eluent. After dried at 35 °C under vacuum overnight to obtain 1.2 g **3**(1) in yellow solid (yield 36%). ^{1}H NMR (300 MHz, $CDCl_3$) δ (ppm): 8.09 (s, 1H, Ar-H *ortho* to OCH_2O), 7.83 (m, 5H, other Ar-H), 6.51, 6.19, 5.90 (m, 3H, C*H*$_2$C*H*CO), 6.07 (s, 2H, OCH_2O), 4.24 (m, 10H, Ar-OC*H*$_2$CH$_2$), 2.02-1.88 (m, 10H, Ar-OCH$_2$C*H*$_2$), 1.65-1.51 (m, 10H, Ar-O(CH$_2$)$_2$C*H*$_2$), 1.48-1.32 (m, 20H, Ar-O(CH$_2$)$_3$(C*H*$_2$)$_2$), 0.94 (t, 15H, J = 6.8 Hz, C*H*$_3$CH$_2$). ESI-MS (*m/z*): $[M + Na]^+$ calcd for $C_{52}H_{76}NaO_8$, 851.54; found, 851.60.

The synthesis of TP-based acrylate monomers **3**(*m*) (*m* = 2, 3, 4, 5) was carried out according to a modified literature procedure.[4,5]

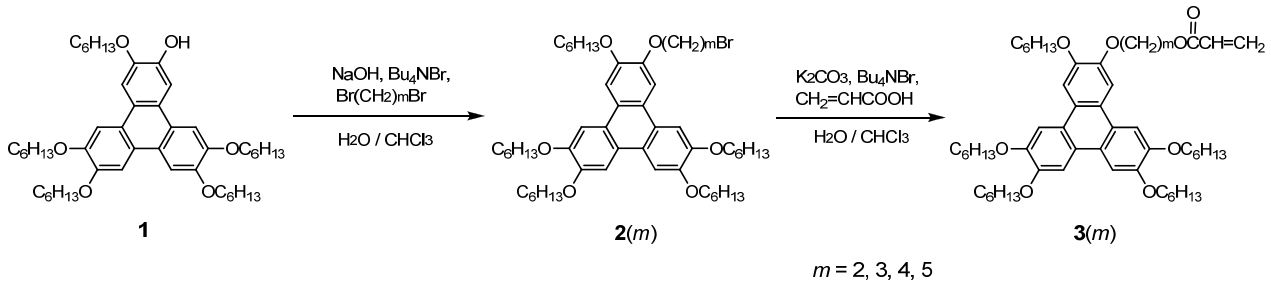

Scheme S3. Synthesis of TP-acrylate monomers **3**(*m*) (*m* = 2–5)

2-(2-bromoethoxy)-3,6,7,10,11-pentakis(hexyloxy)triphenylene (**2**(2))**.** A mixture of **1** (2.4 g, 3.2 mmol), sodium hydroxide (0.26 g, 6.4 mmol), tetrabutylammonium bromide (0.12 g, 0.36 mmol) and 1,2-dibromoethane (2.8 mL, 32 mmol) in 16 mL chloroform and 8 mL water was stirred at room temperature for 18 h. Then the separated organic layer was added 50 mL DCM and washed with 50 mL water. After concentrated under reduced pressure, the crude product was redissolved in minimum DCM and precipitated into 200 mL cold methanol, further through simple filtration and dried at 35 °C under vacuum overnight, 2.2 g intermediate product **2**(2) in yellow solid was collected (yield 80%). ^{1}H NMR (300 MHz, $CDCl_3$) δ (ppm): 7.94 (s, 1H, Ar-H *ortho* to OCH_2CH_2Br), 7.84 (s, 5H, other Ar-H), 4.55 (t, 2H, J = 6.5 Hz, OCH_2CH_2Br), 4.24 (t, 10H, J = 6.4 Hz, $OCH_2(CH_2)_5$), 3.77 (t, 2H, J = 6.5 Hz, CH_2Br), 2.00-1.88 (m, 10H, $OCH_2CH_2CH_2$), 1.66-1.50 (m, 10H, $OCH_2CH_2CH_2$), 1.50-1.32 (m, 20H, $O(CH_2)_3(CH_2)_2CH_3$), 0.94 (t, 15H, J =7.0 Hz, CH_3CH_2).

2-(3,6,7,10,11-pentakis(hexyloxy)triphenylene-2-yloxy)ethyl acrylate (**3**(2))**.** A mixture of **2**(2) (2.2 g, 2.58 mmol), potassium carbonate (6.4 g, 46.4 mmol), acrylic acid (5.0 g, 69.4 mmol), tetrabutylammonium bromide (2.2 g, 6.84 mmol) and a trace amount of hydroquinone in 20 mL chloroform and 40 mL water was stirred at 65 °C for 48 h. The separated organic layer was added 50 mL DCM and washed with 50 mL water. After removal of solvent, the crude product was purified by silica-gel column chromatography using mixed solvent petroleum ether / ethyl acetate (20 : 1, v/v) as the eluent. After dried at 35 °C under vacuum overnight, 1.68 g acrylate monomer **3**(2) in yellow solid was harvested (yield 77%). ^{1}H NMR (300 MHz, $CDCl_3$) δ (ppm): 7.96 (s, 1H, Ar-H *ortho* to OCH_2CH_2OCO), 7.85 (s, 5H, other Ar-H), 6.48, 6.22, 5.86 (m, 3H, CH_2CHCO), 4.65 (t, 2H, J = 5.2 Hz, OCH_2CH_2OCO),

4.50 (t, 2H, J = 5.2 Hz, OCH_2CH_2OCO), 4.24 (t, 10H, J = 6.8 Hz, $OCH_2(CH_2)_5$), 2.01-1.88 (m, 10H, $OCH_2CH_2CH_2$), 1.65-1.51 (m, 10H, $OCH_2CH_2CH_2$), 1.49-1.32 (m, 20H, $O(CH_2)_3(CH_2)_2CH_3$), 0.95 (t, 15H, J = 6.9 Hz, CH_3CH_2). ESI-MS (*m/z*): $[M + Na]^+$ calcd for $C_{53}H_{78}NaO_8$, 865.56; found, 865.70.

2-(3-bromopropoxy)-3,6,7,10,11-pentakis(hexyloxy)triphenylene (**2**(3)). ^{1}H NMR (300 MHz, $CDCl_3$) δ (ppm): 7.90 (s, 1H, Ar-H *ortho* to $OCH_2CH_2CH_2Br$), 7.84 (s, 5H, other Ar-H), 4.40 (t, 2H, J = 5.9 Hz, $OCH_2CH_2CH_2Br$), 4.24 (t, 10H, J = 6.5 Hz, $OCH_2(CH_2)_4$), 3.75 (t, 2H, J = 6.4 Hz, CH_2Br), 2.47 (m, 2H, $OCH_2CH_2CH_2Br$), 2.01-1.88 (m, 10H, $OCH_2CH_2(CH_2)_3$), 1.65-1.52 (m, 10H, $O(CH_2)_2CH_2(CH_2)_2$), 1.48-1.31 (m, 20H, $O(CH_2)_3(CH_2)_2CH_3$), 0.94 (t, 15H, J = 6.9 Hz, CH_2CH_3).

3-(3,6,7,10,11-pentakis(hexyloxy)triphenylene-2-yloxy)propyl acrylate (**3**(3)). ^{1}H NMR (500 MHz, $CDCl_3$) δ (ppm): 7.86 (s, 1H, Ar-H *ortho* to $OCH_2CH_2CH_2OCO$), 7.84 (s, 5H, other Ar-H), 6.43, 6.15, 5.83 (m, 3H, CH_2CHCO), 4.49 (t, 2H, J = 6.5 Hz, $OCH_2CH_2CH_2OCO$), 4.33 (t, 2H, J = 6.0 Hz, CH_2OCO), 4.23 (t, 10H, J = 6.6 Hz, $OCH_2(CH_2)_4$), 2.31 (m, 2H, $OCH_2CH_2CH_2OCO$), 1.98-1.85 (m, 10H, $OCH_2CH_2(CH_2)_3$), 1.62-1.49 (m, 10H, $O(CH_2)_2CH_2(CH_2)_2$), 1.45-1.29 (m, 20H, $O(CH_2)_3(CH_2)_2CH_3$), 0.94 (t, 15H, J = 6.9 Hz, CH_2CH_3). ESI-MS (*m/z*): $[M + Na]^+$ calcd for $C_{54}H_{80}NaO_8$, 879.58; found, 879.70.

2-(4-bromobutoxy)-3,6,7,10,11-pentakis(hexyloxy)triphenylene (**2**(4)). ^{1}H NMR (300 MHz, $CDCl_3$) δ (ppm): 7.84 (s, 6H, Ar-H), 4.24 (t, 12H, J = 6.7 Hz, Ar-O-CH_2), 3.61 (t, 2H, J = 6.3 Hz, CH_2Br), 2.27-2.05 (m, 4H, $OCH_2(CH_2)_2CH_2Br$), 2.01-1.89 (m, 10H, $OCH_2CH_2(CH_2)_4$), 1.65-1.51 (m, 10H, $O(CH_2)_2CH_2(CH_2)_2$), 1.48-1.31 (m, 20H, $O(CH_2)_3(CH_2)_2CH_3$), 0.94 (t, 15H, J = 6.8 Hz, CH_3CH_2).

4-(3,6,7,10,11-pentakis(hexyloxy)triphenylene-2-yloxy)butyl acrylate (**3**(4)). ^{1}H NMR (300 MHz, $CDCl_3$) δ (ppm): 7.85 (s, 6H, Ar-H), 6.43, 6.14, 5.82 (m, 3H, CH_2CHCO), 4.36-4.19 (m, 14H, OCH_2), 2.08-1.89 (m, 14H, OCH_2CH_2), 1.65-1.51 (m, 10H, $O(CH_2)_2CH_2(CH_2)_2$), 1.48-1.32 (m, 20H, $O(CH_2)_3(CH_2)_2CH_3$), 0.94 (t, 15H, J = 6.7 Hz, CH_3CH_2). ESI-MS (*m/z*): $[M + Na]^+$ calcd for $C_{55}H_{82}NaO_8$, 893.59; found, 893.80.

2-(5-bromopentyloxy)-3,6,7,10,11-pentakis(hexyloxy)triphenylene (**2**(5))**.** ^{1}H NMR (500 MHz, $CDCl_3$) δ (ppm): 7.84 (s, 6H, Ar-H), 4.23 (t, 12H, J = 6.9 Hz, OCH_2), 3.48 (t, 2H, J = 6.9 Hz, CH_2Br), 2.06-1.86 (m, 12H, OCH_2CH_2), 1.76 (m, 2H, $BrCH_2CH_2$), 1.62-1.48 (m, 12H, $O(CH_2)_2CH_2$), 1.46-1.25 (m, 20H, $O(CH_2)_3(CH_2)_2CH_3$), 0.94 (t, 15H, J = 6.9 Hz, CH_3CH_2).

5-(3,6,7,10,11-pentakis(hexyloxy)triphenylene-2-yloxy)pentyl acrylate (**3**(5))**.** ^{1}H NMR (500 MHz, $CDCl_3$) δ (ppm): 7.84 (s, 6H, Ar-H), 6.41, 6.13, 5.81 (m, 3H, CH_2CHCO), 4.23 (t, 12H, J = 6.1 Hz, Ar-OCH_2), 4.13 (t, 2H, J = 6.9 Hz, $COOCH_2$), 2.03-1.78 (m, 12H, Ar-OCH_2CH_2), 1.69 (m, 2H, $COOCH_2CH_2$), 1.64-1.47 (m, 12H, Ar-$O(CH_2)_2CH_2$), 1.46-1.19 (m, 20H, Ar-$O(CH_2)_3(CH_2)_2CH_3$), 0.94 (t, 15H, J = 6.8 Hz, CH_3CH_2). ESI-MS (*m/z*): $[M + Na]^+$ calcd for $C_{56}H_{84}NaO_8$, 907.61; found, 907.70.

The synthesis of TP-acrylate monomers **3**(*m*) (*m* = 7–10, 14) was conducted employing the same method as for **3**(6) reported in the previous work.[2]

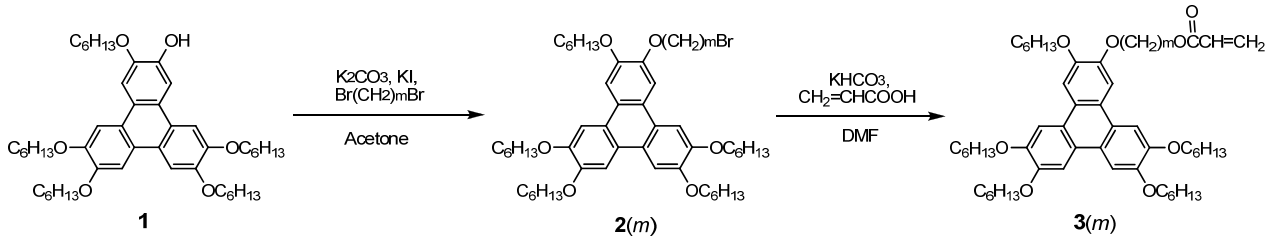

Scheme S4. Synthesis of TP-acrylate monomers **3**(*m*) (*m* = 7–10, 14)

2-(7-bromoheptyloxy)-3,6,7,10,11-pentakis(hexyloxy)triphenylene (**2**(7))**.** ^{1}H NMR (300 MHz, $CDCl_3$) δ (ppm): 7.84 (s, 6H, Ar-H), 4.24 (t, 12H, J = 6.5 Hz, Ar-OCH_2), 3.43 (t, 2H, J = 6.8 Hz, CH_2Br), 2.02-1.82 (m, 14H, Ar-OCH_2CH_2, CH_2CH_2Br), 1.66-1.52 (m, 12H, Ar-$O(CH_2)_2CH_2$), 1.52-1.31 (m, 24H, Ar-$O(CH_2)_3(CH_2)_2$), 0.94 (t, 15H, J = 6.9 Hz, CH_2CH_3).

7-(3,6,7,10,11-pentakis(hexyloxy)triphenylene-2-yloxy)heptyl acrylate (**3**(7))**.** ^{1}H NMR (500 MHz, $CDCl_3$) δ (ppm): 7.84 (s, 6H, Ar-H), 6.4, 6.12, 5.81 (m, 3H, CH_2CHCO), 4.23 (t, 12H, J = 6.5 Hz,

Ar-OCH_2), 4.17 (t, 2H, *J* = 6.7 Hz, $COOCH_2$), 1.99-1.87 (m, 12H, Ar-$OCH_2C\mathit{H_2}$), 1.75-1.67 (m, 2H, $COOCH_2C\mathit{H_2}$), 1.63-1.51 (m, 12H, Ar-$O(CH_2)_2C\mathit{H_2}$), 1.50-1.30 (m, 24H, Ar-$O(CH_2)_3(C\mathit{H_2})_2$), 0.94 (t, 15H, *J* = 7.0 Hz, $CH_2C\mathit{H_3}$). ESI-MS (*m/z*): $[M + Na]^+$ calcd for $C_{58}H_{88}NaO_8$, 935.64; found, 935.70.

2-(8-bromooctyloxy)-3,6,7,10,11-pentakis(hexyloxy)triphenylene (**2**(8))**.** ^{1}H NMR (500 MHz, $CDCl_3$) δ (ppm): 7.84 (s, 6H, Ar-H), 4.23 (t, 12H, *J* = 6.4 Hz, Ar-OCH_2), 3.41 (t, 2H, *J* = 6.9 Hz, $BrCH_2$), 1.98-1.79 (m, 14H, Ar-$OCH_2C\mathit{H_2}$, $BrCH_2C\mathit{H_2}$), 1.62-1.50 (m, 12H, Ar-$O(CH_2)_2C\mathit{H_2}$), 1.47-1.32 (m, 26H, Ar-$O(CH_2)_3(C\mathit{H_2})_2$, $Br(CH_2)_2C\mathit{H_2}$), 0.94 (t, 15H, *J* = 7.0 Hz, $C\mathit{H_3}CH_2$).

8-(3,6,7,10,11-pentakis(hexyloxy)triphenylene-2-yloxy)octyl acrylate (**3**(8))**.** ^{1}H NMR (500 MHz, $CDCl_3$) δ (ppm): 7.84 (s, 6H, Ar-H), 6.40, 6.13, 5.80 (m, 3H, $C\mathit{H_2}C\mathit{H}CO$), 4.23 (t, 12H, *J* = 6.4 Hz, Ar-OCH_2), 4.17 (t, 2H, *J* = 6.5 Hz, $COOCH_2$), 1.99-1.88 (m, 12H, Ar-$OCH_2C\mathit{H_2}$), 1.73-1.65 (m, 2H, $COOCH_2C\mathit{H_2}$), 1.64-1.51 (m, 12H, Ar-$O(CH_2)_2C\mathit{H_2}$), 1.48-1.30 (m, 26H, Ar-$O(CH_2)_3(C\mathit{H_2})_2$, $COO(CH_2)_3C\mathit{H_2}$), 0.94 (t, 15H, *J* = 6.8 Hz, $C\mathit{H_3}CH_2$). ESI-MS (*m/z*): $[M + Na]^+$ calcd for $C_{59}H_{90}NaO_8$, 949.65; found, 949.80.

2-(9-bromononyloxy)-3,6,7,10,11-pentakis(hexyloxy)triphenylene (**2**(9))**.** ^{1}H NMR (300 MHz, $CDCl_3$) δ (ppm): 7.84 (s, 6H, Ar-H), 4.23 (t, 12H, *J* = 6.6 Hz, OCH_2), 3.41 (t, 2H, *J* = 6.8 Hz, $BrCH_2$), 2.01-1.76 (m, 14H, $OCH_2C\mathit{H_2}$, $BrCH_2C\mathit{H_2}$), 1.65-1.51 (m, 12H, $O(CH_2)_2C\mathit{H_2}$), 1.48-1.25 (m, 28H, $O(CH_2)_3(C\mathit{H_2})_2$, $Br(CH_2)_2(C\mathit{H_2})_2$), 0.94 (t, 15H, *J* = 7.0 Hz, $C\mathit{H_3}CH_2$).

9-(3,6,7,10,11-pentakis(hexyloxy)triphenylene-2-yloxy)nonyl acrylate (**3**(9))**.** ^{1}H NMR (300 MHz, $CDCl_3$) δ (ppm): 7.84 (s, 6H, Ar-H), 6.40, 6.13, 5.79 (m, 3H, $C\mathit{H_2}C\mathit{H}CO$), 4.23 (t, 12H, *J* = 6.5 Hz, Ar-OCH_2), 4.16 (t, 2H, *J* = 6.7 Hz, $COOCH_2$), 2.01-1.86 (m, 12H, Ar-$OCH_2C\mathit{H_2}$), 1.74-1.50 (m, 14H, Ar-$O(CH_2)_2C\mathit{H_2}$, $COOCH_2C\mathit{H_2}$), 1.48-1.31 (m, 28H, Ar-$O(CH_2)_3(C\mathit{H_2})_2$, $COO(CH_2)_2(C\mathit{H_2})_2$), 0.94 (t, 15H, *J* = 7.0 Hz, $C\mathit{H_3}CH_2$). ESI-MS (*m/z*): $[M + Na]^+$ calcd for $C_{60}H_{92}NaO_8$, 963.67; found, 963.80.

2-(10-bromodecyloxy)-3,6,7,10,11-pentakis(hexyloxy)triphenylene (**2**(10))**.** ^{1}H NMR (300 MHz, $CDCl_3$) δ (ppm): 7.84 (s, 6H, Ar-H), 4.23 (t, 12H, J = 6.5 Hz, OCH_2), 3.41 (t, 2H, J = 6.9 Hz, $BrCH_2$), 2.00-1.76 (m, 14H, OCH_2CH_2, $BrCH_2CH_2$), 1.65-1.51 (m, 12H, $O(CH_2)_2CH_2$), 1.49-1.22 (m, 30H, $O(CH_2)_3(CH_2)_2$, $Br(CH_2)_2(CH_2)_3$), 0.94 (t, 15H, J = 6.9 Hz, CH_3CH_2).

10-(3,6,7,10,11-pentakis(hexyloxy)triphenylene-2-yloxy)decyl acrylate (**3**(10))**.** ^{1}H NMR (300 MHz, $CDCl_3$) δ (ppm): 7.84 (s, 6H, Ar-H), 6.40, 6.13, 5.82 (m, 3H, CH_2CHCO), 4.23 (t, 12H, J = 6.5 Hz, Ar-OCH_2), 4.16 (t, 2H, J = 6.7 Hz, $COOCH_2$), 2.01-1.88 (m, 12H, Ar-OCH_2CH_2), 1.74-1.50 (m, 14H, Ar-$O(CH_2)_2CH_2$, $COOCH_2CH_2$), 1.49-1.23 (m, 30H, Ar-$O(CH_2)_3(CH_2)_2$, $COO(CH_2)_2(CH_2)_3$), 0.94 (t, 15H, J = 6.9 Hz, CH_3CH_2). ESI-MS (*m/z*): $[M + Na]^+$ calcd for $C_{61}H_{94}NaO_8$, 977.68; found, 977.80.

All α,ω-dibromoalkane were used as received from commercial source except that 1,14-dibromotetradecane was synthesized from tetradecanedioic acid as described below.

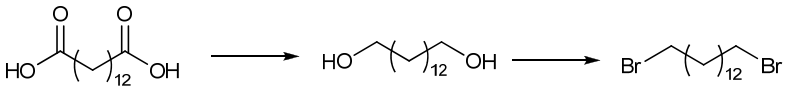

Scheme S5. Synthesis of 1,14-dibromotetradecane from tetradecanedioic acid

1,14-dihydroxytetradecane. This compound was prepared according to the literature.[6] The solution of tetradecanedioic acid (4.5 g, 17.5 mmol) dissolved in 200 mL anhydrous THF was cooled to 0 °C under nitrogen, and 60 mL 1.0 M lithium aluminum hydride solution in THF (60 mmol) was added slowly. The mixture was stirred at 30 °C for 3 h and quenched with ethyl acetate. After added 150 mL water and subsequently acidified with concentrated hydrochloric acid until a clear and transparent solution was gotten, the mixture was extracted twice with ether, dried over anhydrous magnesium sulfate, concentrated and dried at room temperature under vacuum to obtain a white solid, 3.8 g (yield 95%). ^{1}H NMR (500 MHz, $CDCl_3$) δ (ppm): 3.67 (t, 4H, J = 6.4 Hz, $HOCH_2$), 1.59 (m, 4H, $HOCH_2CH_2$), 1.41-1.26 (m, 20H). FT-IR (cm^{-1}): 3405, 3339, 2917, 2848, 1481, 1460, 1371, 1356, 1333, 1053, 1017, 996, 971, 719, 608.

1,14-dibromotetradecane. This compound was prepared according to the literature.[7] A solution of triphenylphosphine (14.9 g, 56.9 mmol) in 100 mL anhydrous THF was added to the solution of *N*-bromosuccinamide (10.1 g, 56.7 mmol) in 100 mL THF at 0 °C, and then another solution of 1,14-dihydroxytetradecane (3.8 g, 16.5 mmol) in 70 mL THF was slowly added to this mixture. The resulting solution mixture was heated to 60 °C for 7 h. After removal of solvent by rotary evaporation, the residue was purified by silica-gel column chromatography with petroleum ether / ethyl acetate (100 : 1, v/v) as the eluent. Then recrystallized from ethanol to obtain a white solid, 2.4 g (yield 41%). ^{1}H NMR (500 MHz, $CDCl_3$) δ (ppm): 3.43 (t, 4H, J = 6.8 Hz, $BrCH_2$), 1.88 (m, 4H, $BrCH_2CH_2$), 1.48-1.25 (m, 20H). FT-IR (cm^{-1}): 2915, 2850, 1472, 1340, 1308, 1259, 1213, 1182, 716, 641.

2-(14-bromotetradecyloxy)-3,6,7,10,11-pentakis(hexyloxy)triphenylene (**2**(14))**.** A mixture of **1** (1.5 g, 2.01 mmol), 1,14-dibromotetradecane (2.4 g, 6.74 mmol), KI (1.6 g, 9.64 mmol) and anhydrous potassium carbonate (6.1 g, 44.1 mmol) in 50 mL acetone was refluxed with stirring for 48 h. The reaction mixture was filtered to remove the inorganic components, then the solvent acetone was removed under reduced pressure. The residue was purified by silica-gel column chromatography with petroleum ether / ethyl acetate (50 : 1, v/v) as the eluent, then dried at 35 °C under vacuum overnight to obtain **2**(14) 1.5 g in yellow solid (yield 73%). ^{1}H NMR (500 MHz, $CDCl_3$) δ (ppm): 7.84 (s, 6H, Ar-H), 4.23 (t, 12H, J = 6.4 Hz, OCH_2), 3.18 (t, 2H, J = 6.9 Hz, $BrCH_2$), 1.94 (m, 12H, OCH_2CH_2), 1.81 (m, 2H, $BrCH_2CH_2$), 1.62-1.50 (m, 12H, $O(CH_2)_2CH_2$), 1.45-1.20 (m, 38H, $O(CH_2)_3(CH_2)_2$, $Br(CH_2)_2(CH_2)_7$), 0.94 (t, 15H, J = 6.8 Hz, CH_3CH_2).

14-(3,6,7,10,11-pentakis(hexyloxy)triphenylene-2-yloxy)tetradecyl acrylate (**3**(14))**.** Acrylic acid (1.5 g, 20.8 mmol) was dropped onto potassium hydrogen carbonate (2.3 g, 23.0 mmol) to form potassium salt of acrylic acid. This mixture was stirred for 10 min prior to the addition of a solution of **2**(14) (1.5 g, 1.47 mmol) in 55 mL DMF and a trace amount of hydroquinone. The resulting mixture was stirred at 120 °C for 24 h. After removal of DMF by rotary evaporation, the residue was dissolved in chloroform and washed twice with water. The solvent was removed under reduced pressure. The residue was purified by

silica-gel column chromatography with petroleum ether / ethyl acetate (40 : 1, v/v) as the eluent. The final product was dissolved in minimum DCM and precipitated into a mixed solution of 250 mL methanol and 50 mL ethanol, then after filtration and dried at 35 °C under vacuum overnight to obtain 0.8 g **3**(14) in yellow solid (yield 54%). ^{1}H NMR (500 MHz, $CDCl_3$) δ (ppm): 7.84 (s, 6H, Ar-H), 6.40, 6.13, 5.82 (m, 3H, C*H*$_2$C*H*CO), 4.23 (t, 12H, *J* = 6.4 Hz, Ar-OC*H*$_2$), 4.15 (t, 2H, *J* = 6.8 Hz, COOC*H*$_2$), 1.99-1.88 (m, 12H, Ar-OCH$_2$C*H*$_2$), 1.66 (m, 2H, COOCH$_2$C*H*$_2$), 1.63-1.50 (m, 12H, Ar-O(CH$_2$)$_2$C*H*$_2$), 1.46-1.21 (m, 38H, Ar-O(CH$_2$)$_3$(C*H*$_2$)$_2$, COO(CH$_2$)$_2$(C*H*$_2$)$_7$), 0.94 (t, 15H, *J* = 6.9 Hz, C*H*$_3$CH$_2$). ESI-MS (m/z): [M + Na]$^+$ for $C_{65}H_{102}NaO_8$, 1033.75; found, 1033.90.

3. Controlled Synthesis of DLCPs by RAFT Polymerization and Their Molecular Characterization

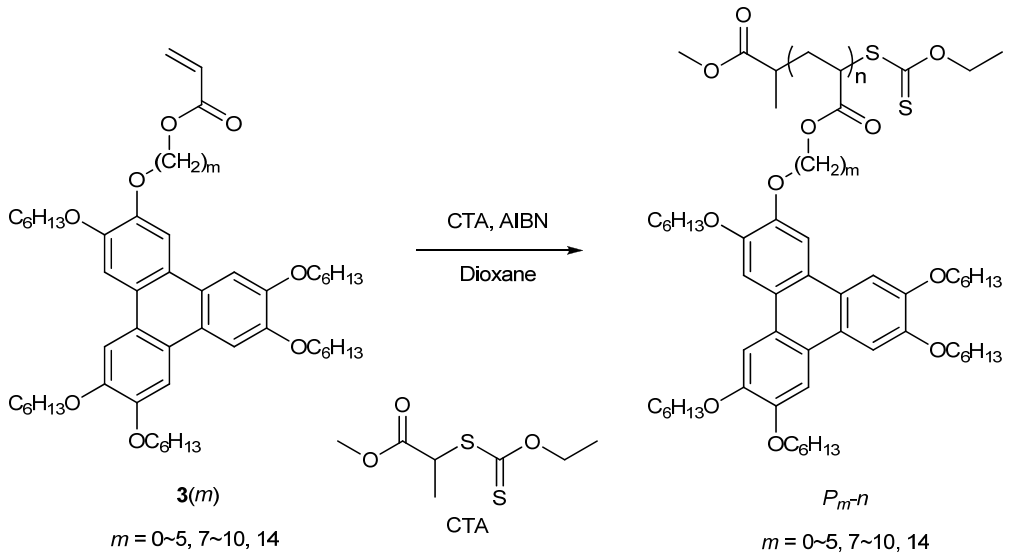

Scheme S6. RAFT polymerization of monomer **3**(*m*) into DLC polyacrylates P_m-*n* with *m* denoting the methylene number of the spacer and *n* for DP of the polymers.

Polymerization procedure for monomers with a medium to long spacer (*m* ≥ 6). The polymerization was conducted with a 50% (w/v) monomer solution in redistilled dioxane (typically 0.6 mL for 0.3 g of monomer) under nitrogen at 60 °C for 45 h in a 10 mL pear-shaped Schlenk flask. AIBN was used as the radical initiator and the molar ratio of AIBN to CTA is 0.5 : 1. The polymerization solution was degassed

by three freeze-pump-thaw cycles before the reaction was initiated. The reaction mixture was purified by silica-gel column chromatography with petroleum ether/ethyl acetate (10 : 1 ~ 20 : 1, v/v) as the eluent first to remove the residual monomer and then the polymer was eluted with ethyl acetate, after concentrated the product was dissolved in DCM and precipitated in cold methanol. Finally the polymer product was dried at 35 °C under vacuum overnight.

Polymerization procedure for monomers with a short spacer ($m \leq 5$). The preparation of oligomers or polymers of lower DPs could be well carried out according to the same protocol as employed for monomers with long spacers. While due to relatively low activity of reactive acrylate groups linked by a short spacer, high-DP polymers could not be obtained with the same experimental conditions. Thus for high-DP polymers of short spacers the polymerization reactions were implemented at elevated temperature 80 °C for 18 h.

Table S1. Molecular characterization results of the family TP-based polyacrylates P_m-n with variant length spacers and DP n = 10 and 50.

polymer code	designed	$M_{n,NMR}$[a]		GPC		
	MW*	***c***[b]	***d***[b]	$M_{w,GPC}$[a]	$M_{n,GPC}$[a]	PDI
P_0-10	8,200	/[d]	/[d]	12,000	8,700	1.37
P_0-50	40,200	/[d]	/[d]	20,400	14,000	1.46
P_1-10	8,500	/[d]	/[d]	9,000	6,900	1.30
P_1-50	41,700	/[d]	/[d]	18,000	12,300	1.46
P_2-10	8,600	/[d]	/[d]	8,100	6,400	1.26
P_2-50	42,400	/[d]	/[d]	11,300	7,900	1.43
P_3-10	8,800	/[d]	/[d]	8,200	6,800	1.21
P_3-50	43,100	/[d]	/[d]	11,700	8,800	1.33
P_4-10	8,900	8,000	9,500	7,900	6,300	1.25
P_4-50	43,800	/[cd]	/[cd]	10,700	8,200	1.30
P_5-10	9,100	7,200	9,000	8,900	7,300	1.22
P_5-50	44,500	/[cd]	/[cd]	13,200	9,800	1.35
P_6-10[e]	9,200	7,400	8,300	8,800	7,100	1.24
P_6-50[e]	45,200	/[c]	46,000	17,000	12,300	1.38
P_7-10	9,300	8,000	9,700	8,800	7,500	1.17
P_7-50	45,900	/[c]	45,000	18,000	13,000	1.38
P_8-10	9,500	8,900	11,000	9,700	8,200	1.18
P_8-50	46,600	/[c]	41,000	17,500	13,200	1.33
P_9-10	9,600	8,400	13,000	10,300	8,700	1.18
P_9-50	47,300	40,000	/[c]	19,000	14,100	1.35
P_{10}-10	9,800	7,000	8,100	12,200	8,900	1.37
P_{10}-50	48,000	/[c]	/[c]	27,000	19,000	1.42
P_{14}-10	10,300	11,000	12,000	12,400	10,300	1.20
P_{14}-50	50,800	43,000	/[c]	30,200	22,800	1.32

[a] Molecular Weight in g mol^{-1}. [b] ***c*** and ***d*** represents different ^{1}H NMR terminal characteristic signal peaks as indicated in Figure S1 adopted as comparative basis for calculating number average molecular weights of the polymers. [c] Not available due to overlapped peaks or too high molecular weight to be estimated by NMR. [d] Not available because of low resolution of the ^{1}H NMR signal peaks as shown in Figure S2, which may result from discotic mesogen-jacketed effect in the liquid crystalline polymers with short spacers. [e] From our previous work as cited in reference 2 (the Ref.10 in main text).

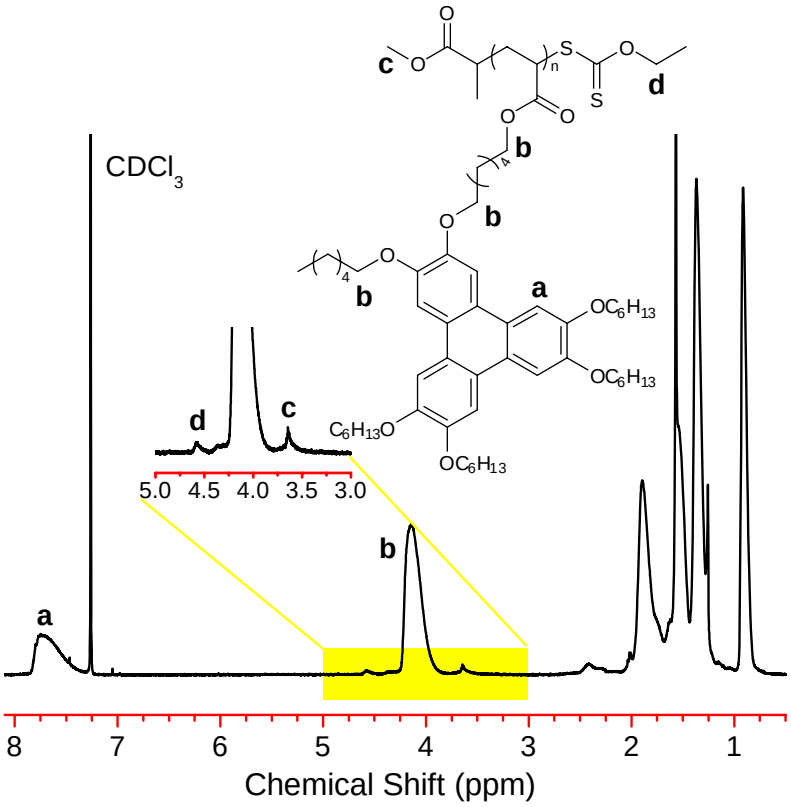

Figure S1. Representative ^{1}H NMR (500 MHz) spectrum of P_6-10

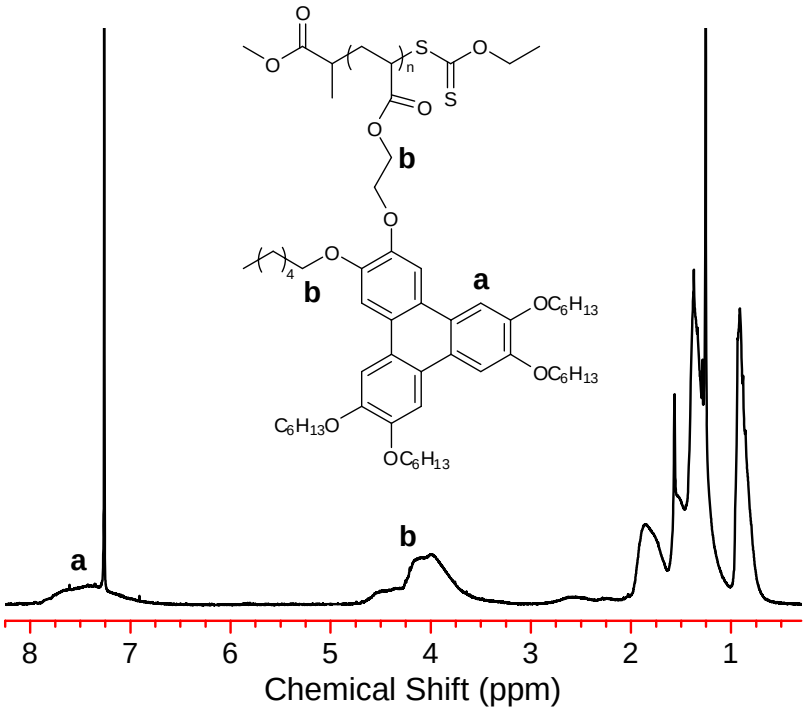

Figure S2. Representative ^{1}H NMR (500 MHz) spectrum of P_2-10 showing broad peaks of low resolution

4. Characterization and Analysis of Variant Self-Organized Superstructures by a Combination of Thermal Analysis and SAXS/WAXS

4.1 Thermal characterization of all related TP-acrylate monomers

Table S2. Thermal transition temperatures and associated enthalpies of all corresponding TP-acrylate monomers of variant length spacers

monomers	phase transitions / °C (enthalpy changes / J g^{-1})[a]		
3(*m*)	first heating[b]	second heating[b]	first cooling[b]
3(0)	K 45(36.2) Col_{ho} 113(5.4) I	Col_{ho} 106(2.1) I	I 99(-1.7) Col_{ho}
3(1)	K 91(69.8) I	K 87(56.8) I	I 59(-58.9) K
3(2)	K 53,62(51.1) I	K 54(34.5) I	I 31(-31.1) K
3(3)	K 59(41.6) Col_{ho} 79(2.5) I	K 59(42.3) Col_{ho} 78(2.8) I	I 76(-2.6) Col_{ho} 40(-41.4) K
3(4)	K 49(44.7) I	K 48(34.6) I	I 30(-34.4) K
3(5)	K 52(52.4) I	K 51(40.9) I	I 31(-39.6) K
3(6)	K 50(49) I	K 47(41) I	I 24(-38) K
3(7)	K_1 50(41.1) K_2 56(0.5) I	K_1 48(44.4) K_2 55(3.4) I	I 35(-2.8) K_2 29(-42.5) K_1
3(8)	K 56(63.1) I	K 54(59.2) I	I 32(-2.9) 28(-48.0) K
3(9)	K 53(63.3) I	K 48(53.8) I	I 27(-49.8) K
3(10)	K 46(48.2) I	K 42(44.2) I	I 22(-42.8) K
3(14)	K_1 35(27.0) K_2 44(10.2) I	K 32,35(34.8) I	I 18(-36.2) K

[a] Abbreviations: K = crystalline phase; Col_{ho} = ordered hexagonal columnar mesophase; I = isotropic phase. [b] The transition peak values obtained from DSC heating or cooling runs at a rate of 10 °C min^{-1}, with positive enthalpy changes standing for endothermic while negative values for exothermic transitions.

4.2 Representative POM textures of DLCPs

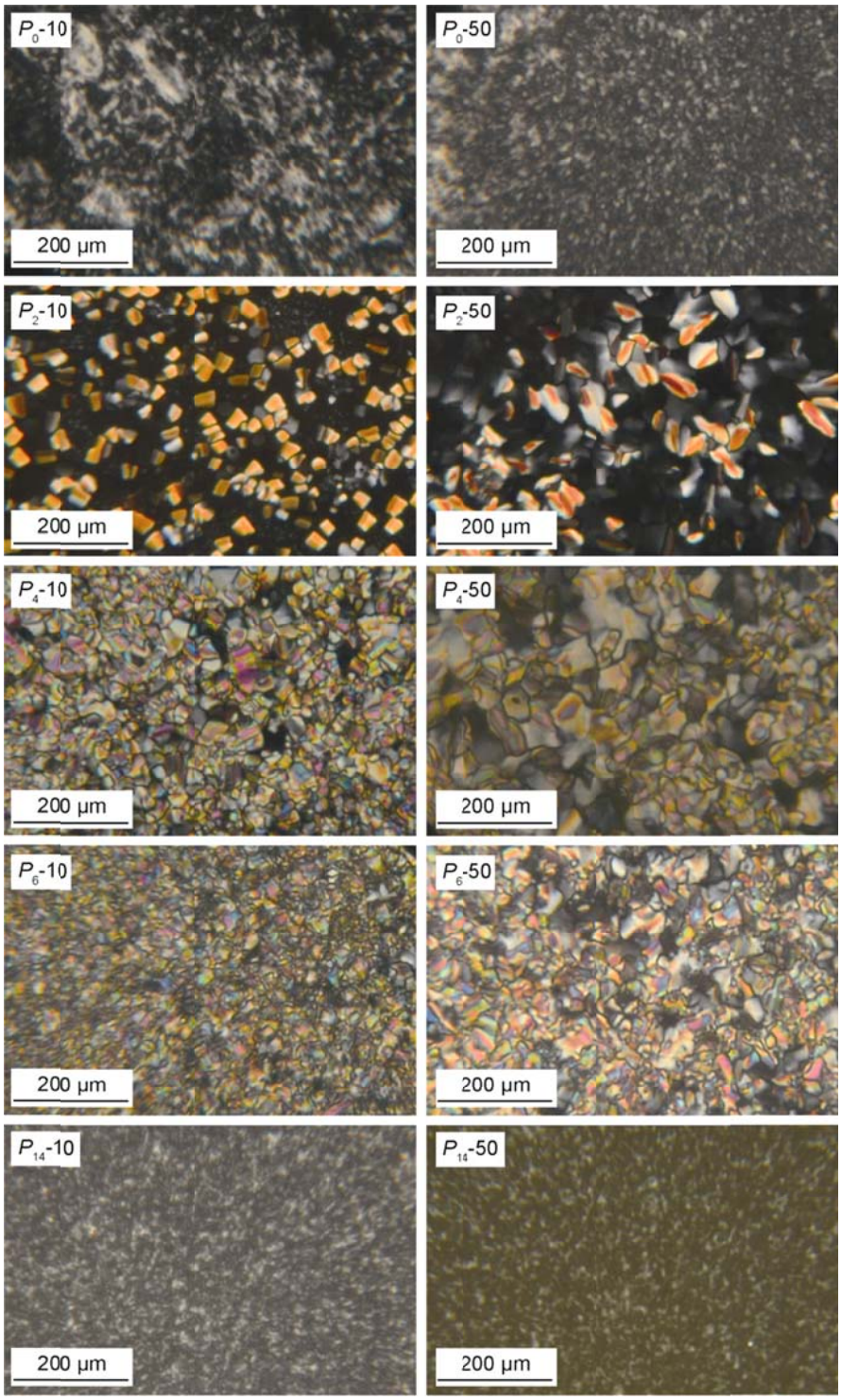

Figure S3. Representative POM images under crossed polarizers of P_m-n at room temperature after slowly cooling from the isotropic state.

4.3 SAXS/WAXS Characterization and Analysis for P_0-n

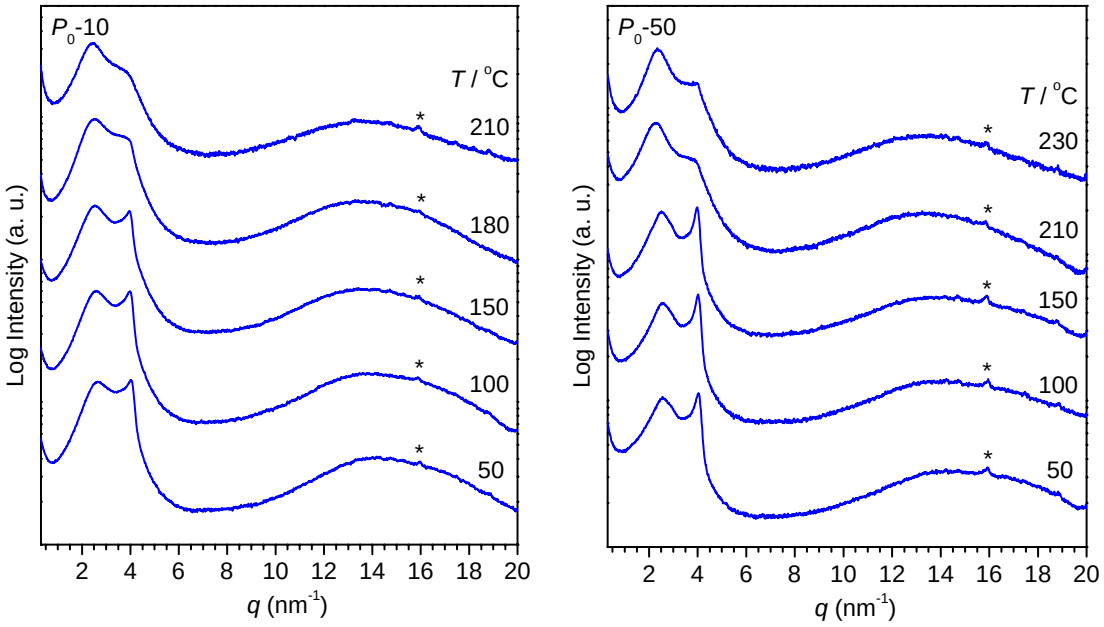

Figure S4. Variable temperature SAXS/WAXS patterns of P_0-n at indicated temperatures during the subsequent heating process after cooling from isotropic melts at 10 °C min^{-1}.

*The background peaks from the packing aluminum foil locating in the wide-angle region are labeled by asterisks, which have a negligible disturbance to the interested sample peaks thus without complete subtraction so as to avoid distortion of the peak shape and smoothing over some significant weak signals, *hereinafter the same*.

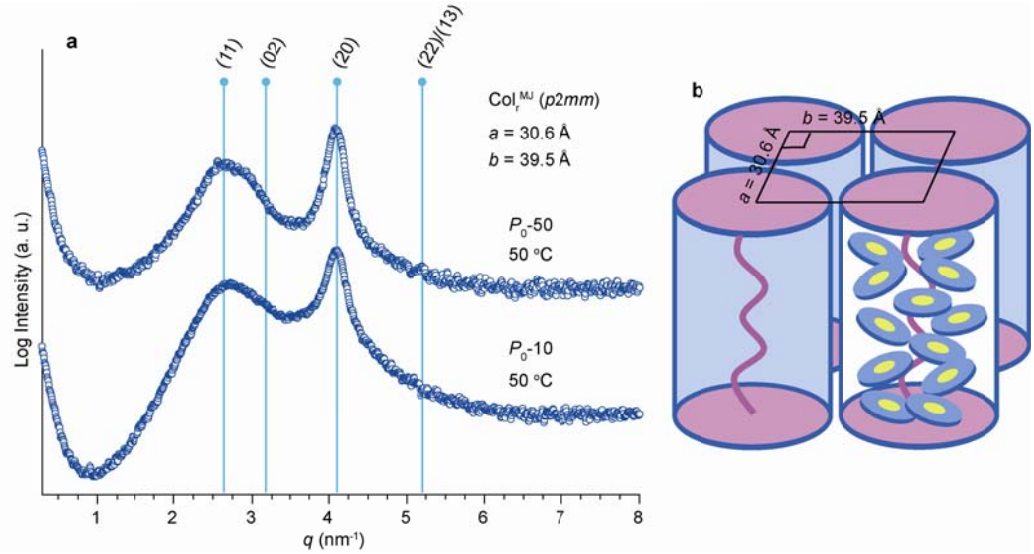

Figure S5. (a) SAXS patterns of P_0-10 and P_0-50 with proposed indexing at 50 °C after cooling from isotropic melts at 10 °C min^{-1}. (b) Schematic illustration of rectangular columnar lattice Col$_r^{MJ}$ (*p*2*mm*) organized by discotic mesogen-jacketed LCPs without a flexible spacer of P_0-*n*.

Both P_0-*n* exhibited no thermal transition with detectable enthalpy change in either heating or cooling scans of DSC tests, while variable temperature POM observation and temperature dependent SAXS/WAXS analyses rendered their melting transition temperatures. As shown in Figure S4, the SAXS/WAXS profiles of P_0-10 and P_0-50 showed similar patterns, with only a diffuse halo centered at 4.3 Å in the WAXS region corresponding to liquid-like aliphatic chains, and two strong SAXS reflections in the low angle region. Their clearing temperatures of melting into the isotropic state were determined to be higher than 210 °C for P_0-10 and over 230 °C for P_0-50 from temperature dependent SAXS analyses. All the thermal performance and structural characteristics were reminiscent of discotic mesogen-jacketed LCPs with rigid polyacetylene backbone and short spacers[8] or conventional calamitic mesogen-jacketed LCPs.[9] A rectangular columnar phase Col$_r^{MJ}$ (*p*2*mm*) with lattice parameter a = 30.6 Å and b = 39.5 Å could be tentatively assigned from the main reflections (Figure S5a) with detailed data summarized in Table S3, with referring to the rectangular columnar phase assignment of TP-based side-chain discotic LCPs with no flexible spacer and with polymethacrylate backbone.[10] It was proposed that the flexible polymer backbone was closely wrapped by discotic mesogens, thus resulted in a stretched polymer chain in a rigid supramolecular cylinder shape which acted as the building block for constructing 2D columnar

lattice (Figure S5b). The estimated lattice spacings agreed well with the cross section dimension of the supramolecular column of hexyloxy substituted TP based mesogen-jacketed LC polyacetylenes (a = 34.5 Å of hexagonal lattice) and their tendency to transform from hexagonal to rectangular columnar structure with shortened spacers.[8] Though other possibilities cannot be completely precluded at present due to the poor resolution of higher order reflections, it is sure enough and fortunate that some uncertainty in determining the 2D lattice of the unique discotic mesogen-jacketed P_0-n samples has no substantial influence on ascertaining the structures of other polymers with variant length flexible spacers and understanding the role of spacer for the homologous series side-chain DLCPs.

Table S3. SAXS/WAXS data for P_0-n at 50 °C after cooling from the isotropic state at 10 °C min^{-1}.

mesophase	*hkl*	d_{obs} [Å]	d_{cacl} [Å]	lattice parameter [Å]	ρ_{calc}
Col_r^{MJ}	110	2.42	2.42	a = 30.6	/
(50 °C)	020	1.98	1.98	b = 39.5	
p2mm	200	1.53	1.53		
	220/130	1.21	1.21		
		4.30 (diffuse halo)			

4.4 SAXS/WAXS Characterization and Analysis for P_1-*n*

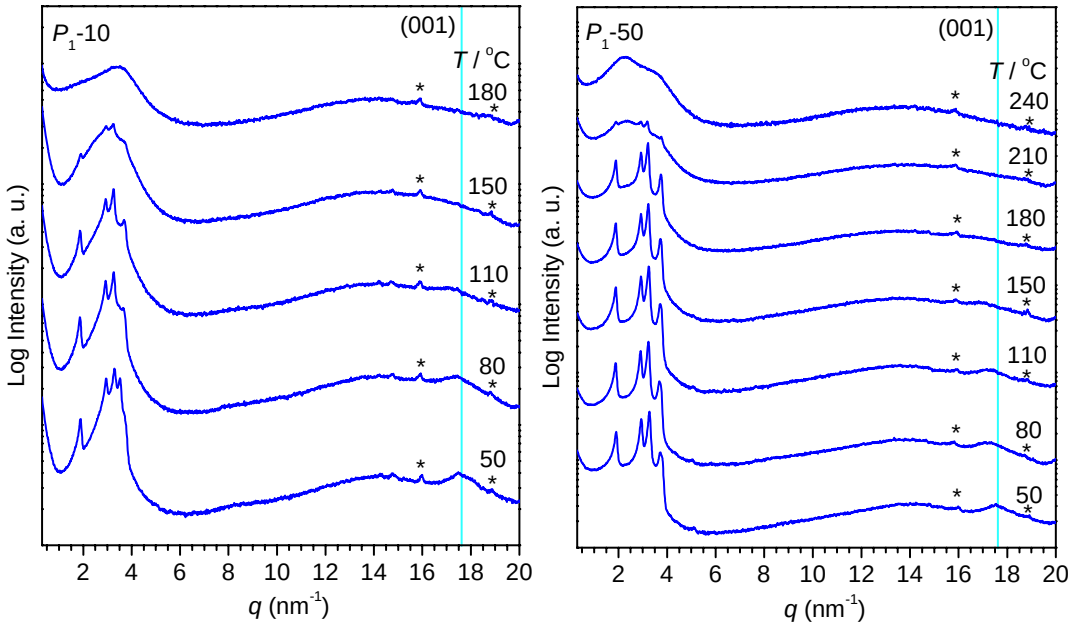

Figure S6. Variable temperature SAXS/WAXS patterns of P_1-*n* at indicated temperatures during the subsequent heating process after cooling from isotropic melts at 10 °C min^{-1}.

Table S4. SAXS/WAXS data for P_1-*n* at 50 °C after cooling from the isotropic state at 10 °C min^{-1}.

mesophase	*hkl*	d_{obs} [Å]	d_{cacl} [Å]	lattice parameter [Å]	ρ_{calc} [a]
Col_{ob-s}	100	32.9	32.9	a = 33.1	1.09
(50 °C)	010	21.4	21.4	b = 21.6	g cm^{-3}
*p*2	110	19.0	19.0	γ = 83.2°	
	1-10	17.0	17.0		
	200	16.5	16.5		
	210	14.0	13.9		
	2-10	12.3	12.3		
	120	10.6	10.5		
		4.49 (diffuse halo)			
	001	3.56			

[a] The calculated density ρ_{calc} based on measured lattice parameters was determined as $\rho = M \cdot Z/(N_A \cdot V_{unit\ cell})$, where $V_{unit\ cell}(Col_{ob-s}) = a \cdot b \cdot \sin\gamma \cdot c$, Z = 2 (c = 3.56 Å), and M is the molecular weight of the repeat unit of 829 g mol^{-1}.

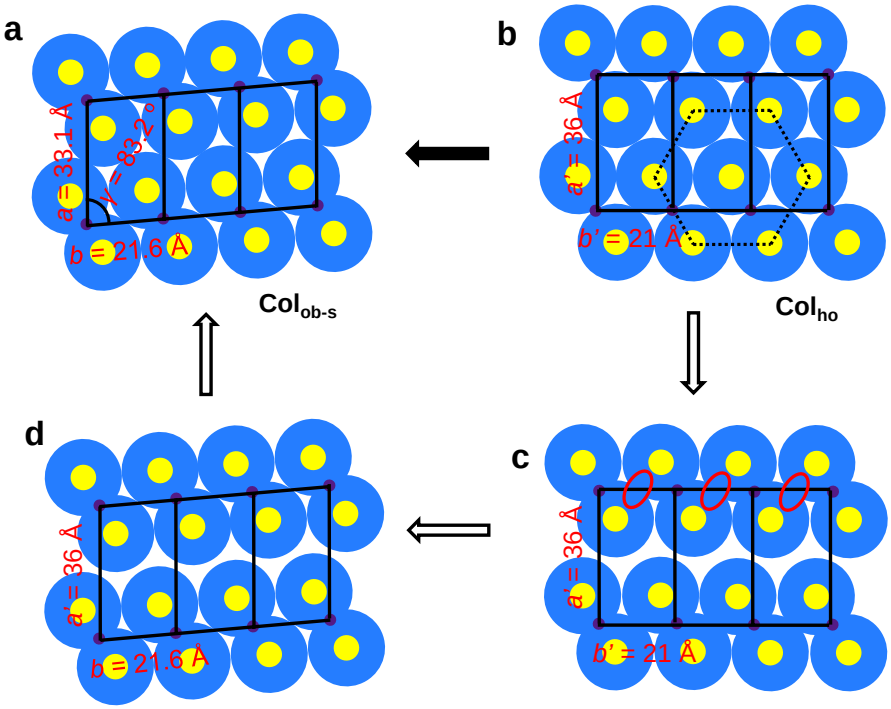

Figure S7. (a) Schematic illustration of oblique columnar superlattice Col$_{ob-s}$ (*p*2) based on "twin-column" bundles in the shortest spacer series P_1-*n* and its proposed evolution pathway from (b) the ordered hexagonal columnar lattice adopted by analogous DLCP with longer spacers dominated by TP-stacking to (c) gradually distorted due to its too short spacer length and further with (d) horizontally intralayer and (a) vertically interlayer adjustment to alleviate the steric hindrance and reach potential closest packing superlattice structure in P_1-*n* series.

Structure evolution of P_1-*n* from Col$_{ho}$ to Col$_{ob-s}$ based on geometric consideration (Figure 1b in the main text) of backbone identity period of 2.5 Å in an all *trans* conformation smaller than the determined intra-columnar distance of about 3.56 Å, and the maximum horizontal distance between two neighboring discogens in the same polymer chain was estimated to be (3.7 + 6.0) × 2 = 19.4 Å assuming an all *trans* conformation of spacers, which was obviously shorter than the measured inter-columnar distance of about 21 Å from hexyloxy substituted TP stacking,[2] thus the pendant TP discogens attached on a polymer backbone could not afford to construct different columns and most probably stacked alternately at opposite sides of the backbone axis to form "twin-column" bundles with partly overlapping of peripheral alkoxy side chains. Then the "twin-column" bundles as building blocks further organized into 2D oblique

superlattice with geometric dimensions showing great accordance with the measured lattice parameters and justified as illustrated in Figure S7. Starting from the most preferred packing of 2D hexagonal columnar lattice (Figure S7b) by TP-stacking of low molar mass discogens[11,12] or analogous polymers with longer spacers as demonstrated in P_6-n series,[2] marked steric hindrance among adjacent bundles as indicated by red circles (Figure S7c) would occur with too short spacers to link two opposite columns in the same a polymer chain, resulting in obvious overlapping or partial merging of these twin-columns, assuming preserving the Col_{ho} with relatively fixation of polymer main chain positions upon adopting a very short spacer. Therefore, some adjustments within horizontally intralayer (Figure S7d) and among vertically interlayer (Figure S7a) have to take place to alleviate the steric hindrance and realize potential closest packing of "twin-column" bundles. Such an adjustment and optimization led to an oblique 2D superlattice $Col_{ob\text{-}s}$ of a = 33.1 Å and b = 21.6 Å, with a remarkable shrinkage in the vertical direction while a little expansion in the horizontal direction as compared with a' = 36.0 Å and b' = 21.0 Å of the virtual rectangular superlattice of polymer backbone in Col_{ho} structure by TP stacking, and slight change from a right-angle to the angle γ = 83.2° between a and b manifested a slightly distorted while more compact oblique superlattice organization.

4.5 SAXS/WAXS Characterization and Analysis for P_2-*n*

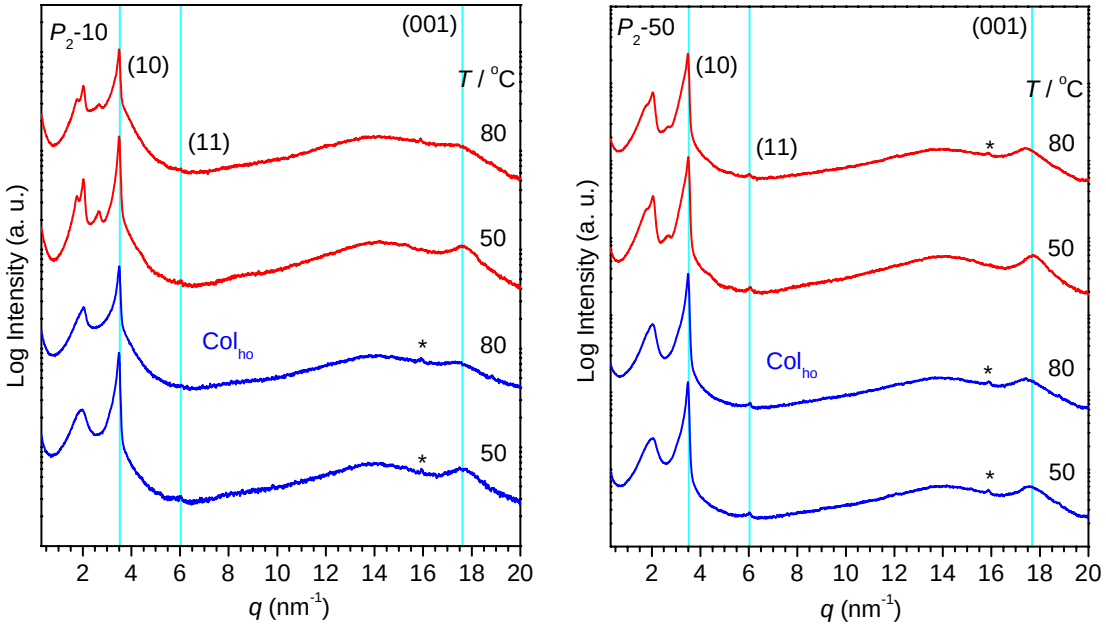

Figure S8. Variable temperature SAXS/WAXS patterns of P_2-*n* at indicated temperatures during the subsequent heating process after cooling from isotropic melts at a rate of 10 °C min^{-1} (blue lines) or through a stepwise cooling process (red lines), wherein the *stepwise cooling* process was performed through isothermal annealing at a set of selected tempeartures about 10 °C interval step-down from isotropic melts to room temperature, essentially equivalent to a very slow cooling process, hereinafter the same.

Table S5. SAXS/WAXS data for P_2-*n* at 50 °C after a stepwise cooling process

mesophase	*hkl*	d_{obs} [Å]	d_{cacl} [Å]	lattice parameter [Å]	ρ_{calc} [a]
Col_{r-s}	100	36.0	36.0	a = 36.0	1.07
(50 °C)	110/020[b]	30.8	30.8/30.8	b = 61.6	g cm^{-3}
*p*2	120	23.3	23.4		
	130/200	18.0	18.0/18.0		
	140	14.1	14.1		
	150/310	11.7	11.6/11.8		
	330	10.3	10.3		
		4.48 (diffuse halo)			
	001	3.54			

[a] The density, ρ, was calculated as $\rho = M{\cdot}Z/(N_A{\cdot}V_{unit\ cell})$, where $V_{unit\ cell}(Col_{r-s}) = a{\cdot}b{\cdot}c$, Z = 6 (c = 3.54 Å), and M is the molecular weight of the repeat unit of 843 g mol^{-1}. [b] This indexation satisfying an additional extinction rule of (0k): $k = 2i + 1$ (i is an integer) in a simple 2D rectangular *p*2 lattice.

4.6 SAXS/WAXS Characterization and Analysis for P_3-*n*

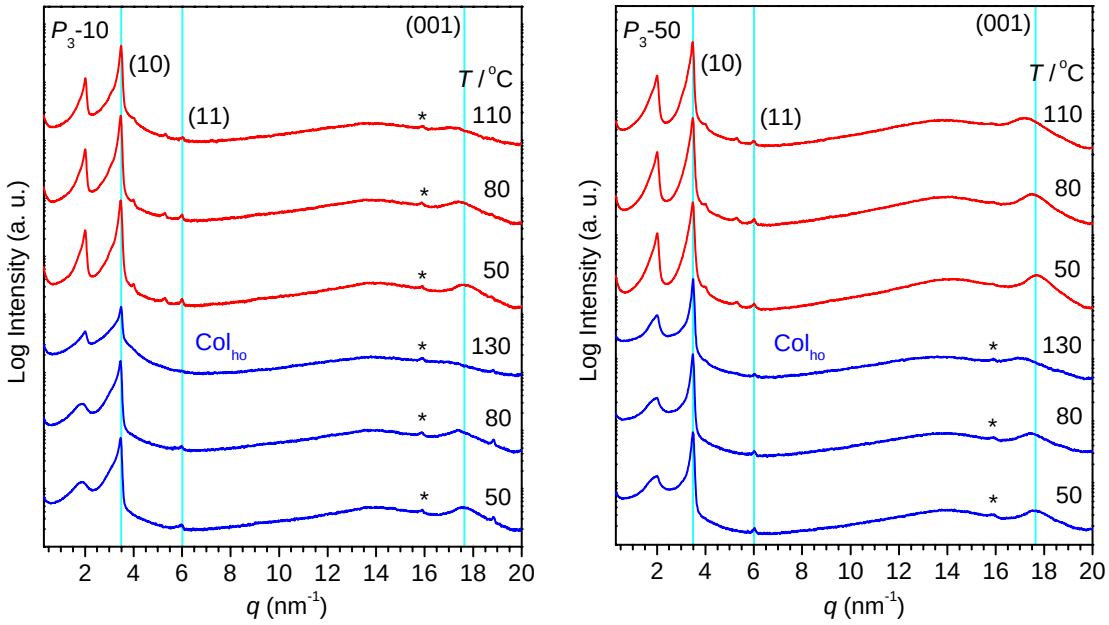

Figure S9. Variable temperature SAXS/WAXS patterns of P_3-*n* at indicated temperatures during the subsequent heating process after cooling from isotropic melts at a rate of 10 °C min^{-1} (blue lines) or through a stepwise cooling process (red lines).

Table S6. SAXS/WAXS data for P_3-*n* at 50 °C after a stepwise cooling process

mesophase	*hkl*	d_{obs} [Å]	d_{cacl} [Å]	lattice parameter [Å]	ρ_{calc} [a]
$Col_{h\text{-}s}$	100	31.0	31.0	a = 35.8	1.08
(50 °C)	110	18.0	17.9		g cm^{-3}
*p*3*m*1	200	15.5	15.5		
	120	11.8	11.7		
	300	10.4	10.3		
		4.44 (diffuse halo)			
	001	3.55			

[a] The density, ρ, was calculated as $\rho = M{\cdot}Z/(N_A{\cdot}V_{unit\ cell})$, where $V_{unit\ cell}(Col_{h\text{-}s}) = a^2{\cdot}c{\cdot}\sqrt{3}/2$, Z = 3 (c = 3.55 Å), and M is the molecular weight of the repeat unit of 857 g mol^{-1}.

4.7 SAXS/WAXS Characterization and Analysis for P_4-*n* and P_5-*n*

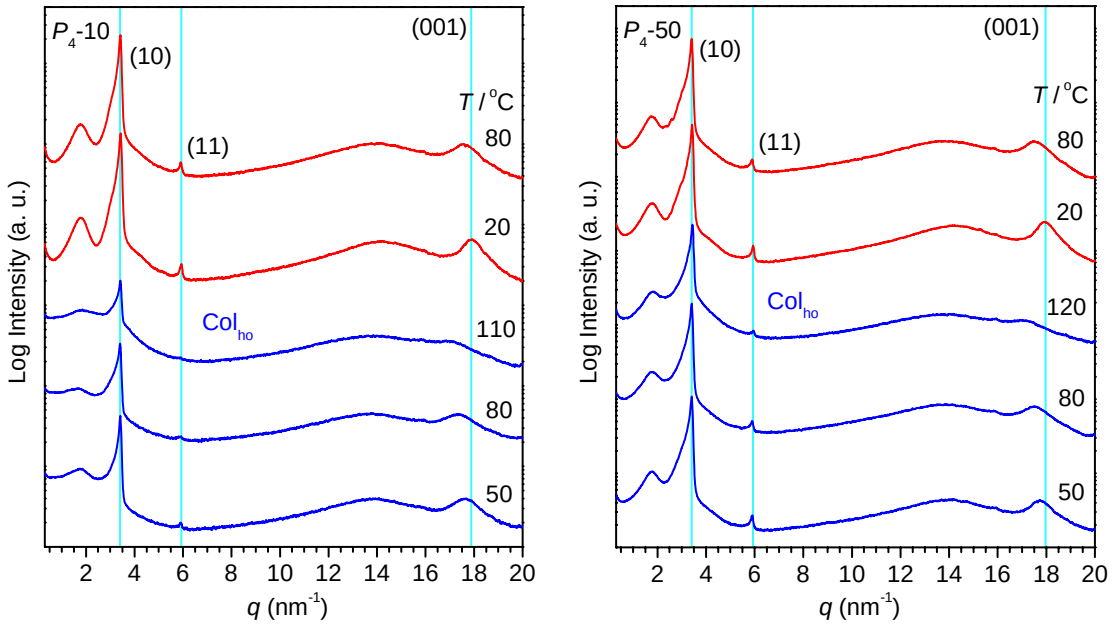

Figure S10. Variable temperature SAXS/WAXS patterns of P_4-*n* at indicated temperatures during the subsequent heating process after cooling from isotropic melts at a rate of 10 °C min^{-1} (blue lines) or through a stepwise cooling process (red lines).

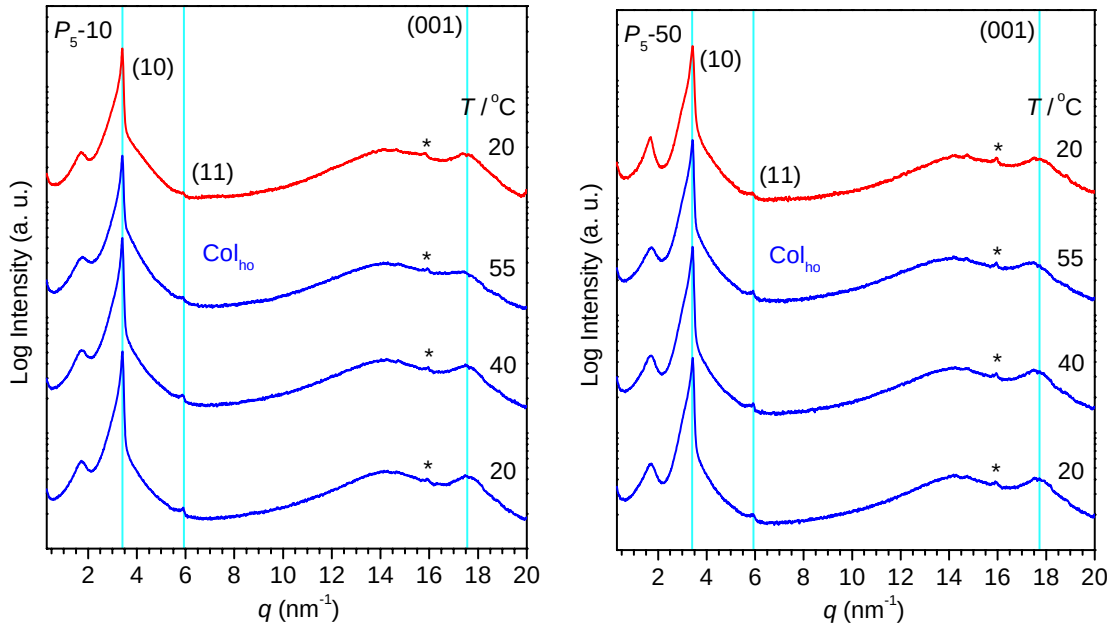

Figure S11. Variable temperature SAXS/WAXS patterns of P_5-*n* at indicated temperatures during the subsequent heating process after cooling from isotropic melts at a rate of 10 °C min^{-1} (blue lines) or through a stepwise cooling process (red lines).

Table S7. SAXS/WAXS data for P_4-*n* and P_5-*n* at 20 °C after a stepwise cooling process

mesophase	*hkl*	d_{obs} [Å]	d_{cacl} [Å]	lattice parameter [Å]	ρ_{calc} [a]
Col_{ho}/L	L =1	36.7	36.6	L = 36.7	1.07
(20 °C)	100 (L =2)	18.3	18.3	a = 21.1	g cm^{-3}
p1	110	10.6	10.6		
	001	4.39 (diffuse halo) 3.49 for P_4-*n* 3.55 for P_5-*n*			

[a] The densities, ρ, were calculated as $\rho = M{\cdot}Z/(N_A{\cdot}V_{unit\ cell})$, where $V_{unit\ cell}(Col_{ho}/L) = a^2{\cdot}c{\cdot}\sqrt{3}/2$, Z = 1 (c = 3.49 Å for P_4-*n* and 3.55 Å for P_5-*n*), and M is the molecular weights of the repeat unit of 871 g mol^{-1} for P_4-*n* and 885 g mol^{-1} for P_5-*n*, respectively.

4.8 SAXS/WAXS Characterization and Analysis for P_7-*n* and P_8-*n*

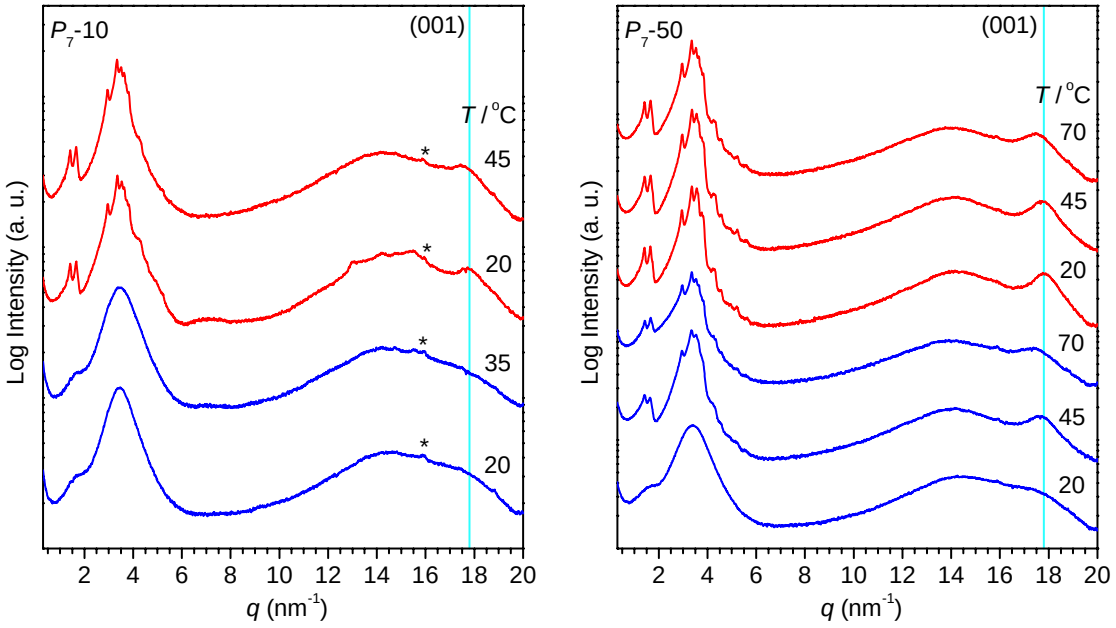

Figure S12. Variable temperature SAXS/WAXS patterns of P_7-*n* at indicated temperatures during the subsequent heating process after cooling from isotropic melts at a rate of 10 °C min^{-1} (blue lines) or through a stepwise cooling process (red lines).

Table S8. SAXS/WAXS data for P_7-*n* after a stepwise cooling process

mesophase	*hkl*	d_{obs} [Å]	d_{cacl} [Å]	lattice parameter [Å]	ρ_{calc} [a]
Col_{ob-s}	200	44.3	44.3	a = 88.5	0.92
(20 °C)	110	38.4	38.5	b = 42.5	g cm^{-3}
*p*2	020	21.3	21.3	γ = 89.0°	
	220	19.0	19.3		
	320	17.6	17.4		
	3-20	17.2	17.1		
	510	16.4	16.4		
	600	14.6	14.8		
	520	13.7	13.7		
	330	12.7	12.9		
	430/6-20	12.0	12.0/12.0		
	800	11.1	11.1		
		4.38 (diffuse halo)			
	001	3.52			

[a] The density, ρ, was calculated as $\rho = M \cdot Z/(N_A \cdot V_{unit\ cell})$, where $V_{unit\ cell}(Col_{ob-s}) = a \cdot b \cdot \sin\gamma \cdot c$, Z = 8 (c = 3.52 Å), and M is the molecular weight of the repeat unit of 913 g mol^{-1}.

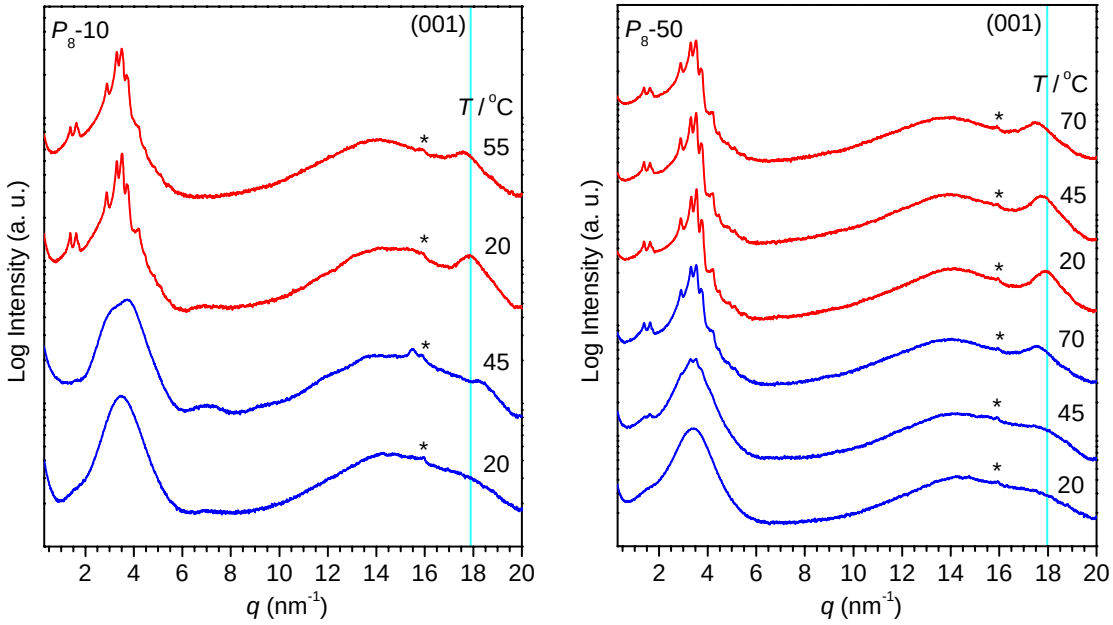

Figure S13. Variable temperature SAXS/WAXS patterns of P_8-*n* at indicated temperatures during the subsequent heating process after cooling from isotropic melts at a rate of 10 °C min^{-1} (blue lines) or through a stepwise cooling process (red lines).

Table S9. SAXS/WAXS data for P_8-*n* after a stepwise cooling process

mesophase	*hkl*	d_{obs} [Å]	d_{cacl} [Å]	lattice parameter [Å]	ρ_{calc} [a]
$Col_{r\text{-}s}$	200 [b]	45.2	45.2	a = 90.4	0.90
(20 °C)	110	38.3	38.3	b = 43.0	g cm^{-3}
*p*2*gg*	020 [b]	21.5	21.2		
	220	19.3	19.2		
	320	17.4	17.3		
	510	16.6	16.6		
	600 [b]	15.0	15.1		
	130	13.9	13.9		
	330	12.8	12.8		
	620	12.2	12.3		
	800 [b]	11.3	11.3		
		4.38 (diffuse halo)			
	001	3.51			

[a] The density, ρ, was calculated as $\rho = M \cdot Z/(N_A \cdot V_{unit\ cell})$, where $V_{unit\ cell}(Col_{r\text{-}s}) = a \cdot b \cdot c$, Z = 8 (c = 3.51 Å), and M is the molecular weight of the repeat unit of 927 g mol^{-1}. [b] This indexation is consistent with the extinction rule of a 2D rectangular *p*2*gg* lattice: (h0): $h = 2i + 1$, 0k: $k = 2i + 1$.

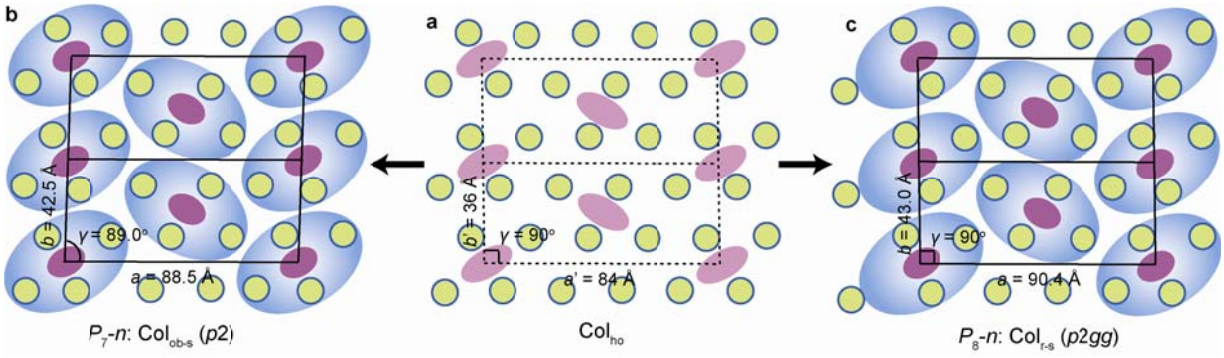

Figure S14. Structure evolution of P_7-*n* and P_8-*n* from (a) Col_{ho} to (b) $Col_{ob\text{-}s}$ or (c) $Col_{r\text{-}s}$, respectively.

To elucidate the detailed organization structure of P_7-*n* and P_8-*n*, assuming polymer main chains' locations on the basis of 2D hexagonal columnar lattice dominated by TP stacking as mostly adopted by similar polymers (Figure S14a), the calculated values for virtual rectangular superlattice of a' = 84 Å, b' = 36 Å were particularly close to the experimentally determined lattice parameters with P_7-*n* of a = 88.5 Å, b = 42.5 Å, γ = 89.0° (Figure S14b) and P_8-*n* of a = 90.4 Å, b = 43.0 Å, γ = 90° (Figure S14c), which implied that both $Col_{ob\text{-}s}$ and $Col_{r\text{-}s}$ superlattices resulted from a little distortion of original hexagonal lattice disturbed by non-mesogenic moieties of main chain and slightly overlong spacers.

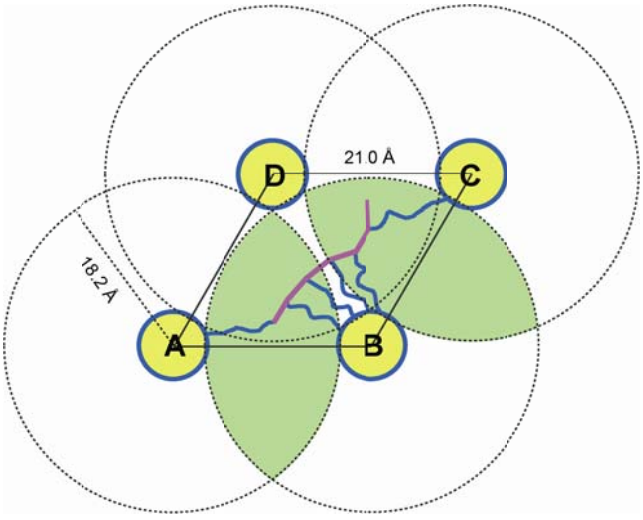

Figure S15. Schematic illustration to show geometric dimensions and arrangement of the polymer main chain and pendant TP discogens in polyacrylate P_8-*n*.

4.9 SAXS/WAXS Characterization and Analysis for P_9-*n*

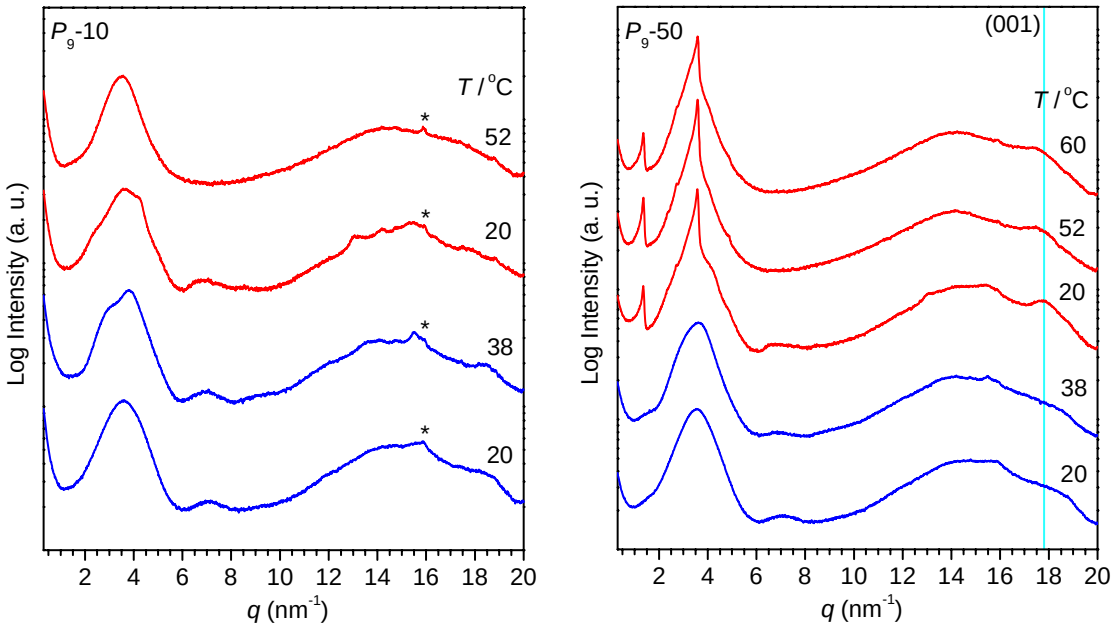

Figure S16. Variable temperature SAXS/WAXS patterns of P_9-*n* at indicated temperatures during the subsequent heating process after cooling from isotropic melts at a rate of 10 °C min^{-1} (blue lines) or through a stepwise cooling process (red lines).

Table S10. SAXS/WAXS data for P_9-50 after a stepwise cooling process

mesophase	*hkl*	d_{obs} [Å]	d_{cacl} [Å]	lattice parameter [Å]	ρ_{calc}[a]
$Col_{h\text{-}s}$	100	46.5	46.5	a = 53.7	1.07
(20 °C)	110	26.7	26.8		g cm^{-3}
p6mm	200	23.3	23.3		
	120	17.5	17.6		
	300	15.5	15.5		
	130	12.8	12.9		
		4.37 (diffuse halo)			
	001	3.52			

[a] The density, ρ, was calculated as $\rho = M{\cdot}Z/(N_A{\cdot}V_{unit\ cell})$, where $V_{unit\ cell}(Col_{h\text{-}s}) = a^2{\cdot}c{\cdot}\sqrt{3}/2$,, Z = 6 (c = 3.52 Å), and M is the molecular weight of the repeat unit of 941 g mol^{-1}.

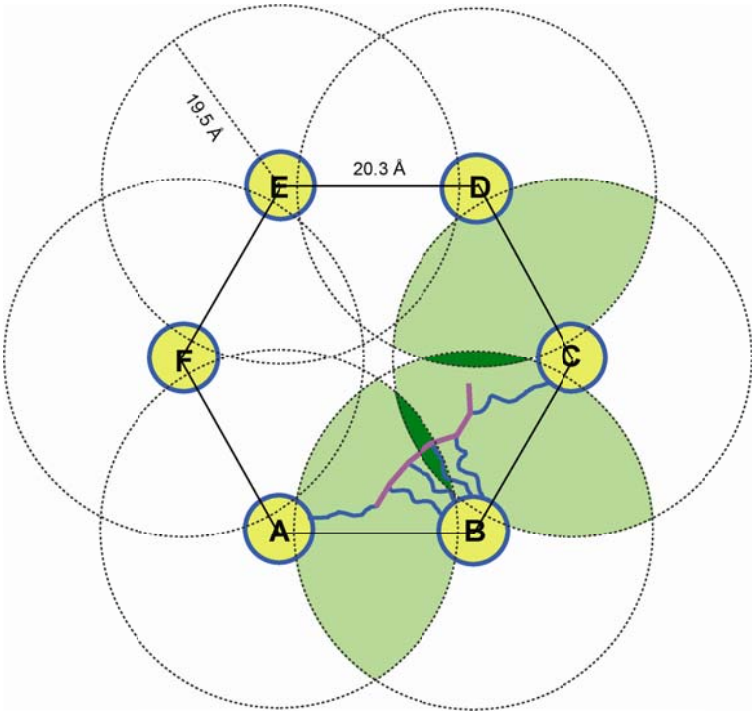

Figure S17. Schematic illustration to show geometric dimensions and arrangement of the polymer main chain and pendant TP discogens in polyacrylate P_9-*n*.

4.10 SAXS/WAXS Characterization and Analysis for P_{10}-*n* and P_{14}-*n*

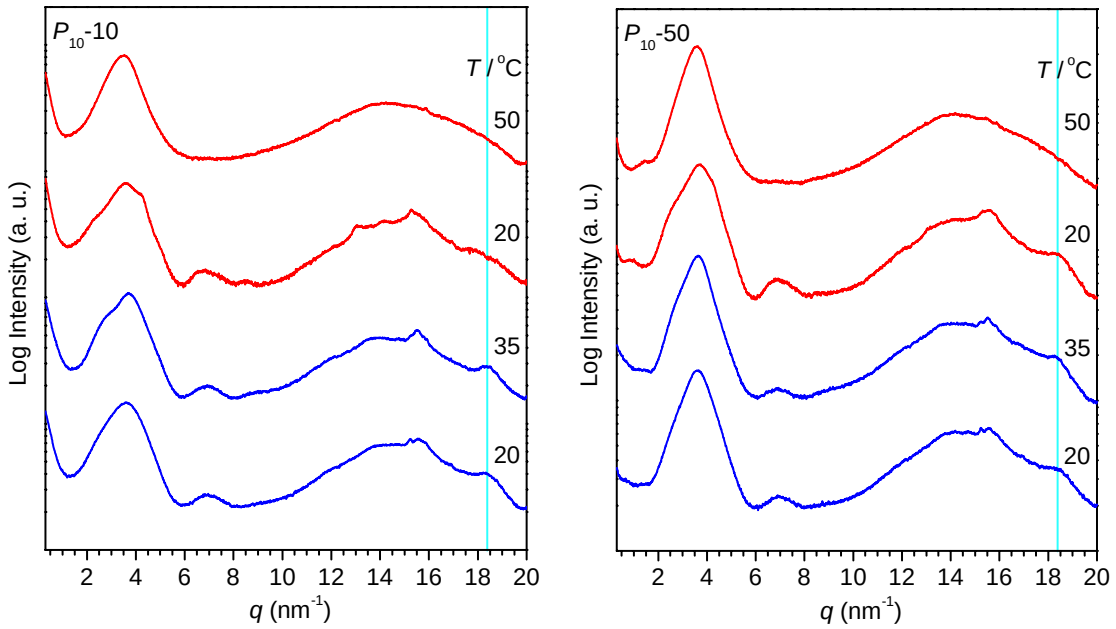

Figure S18. Variable temperature SAXS/WAXS patterns of P_{10}-*n* at indicated temperatures during the subsequent heating process after cooling from isotropic melts at a rate of 10 °C min^{-1} (blue lines) or through a stepwise cooling process (red lines).

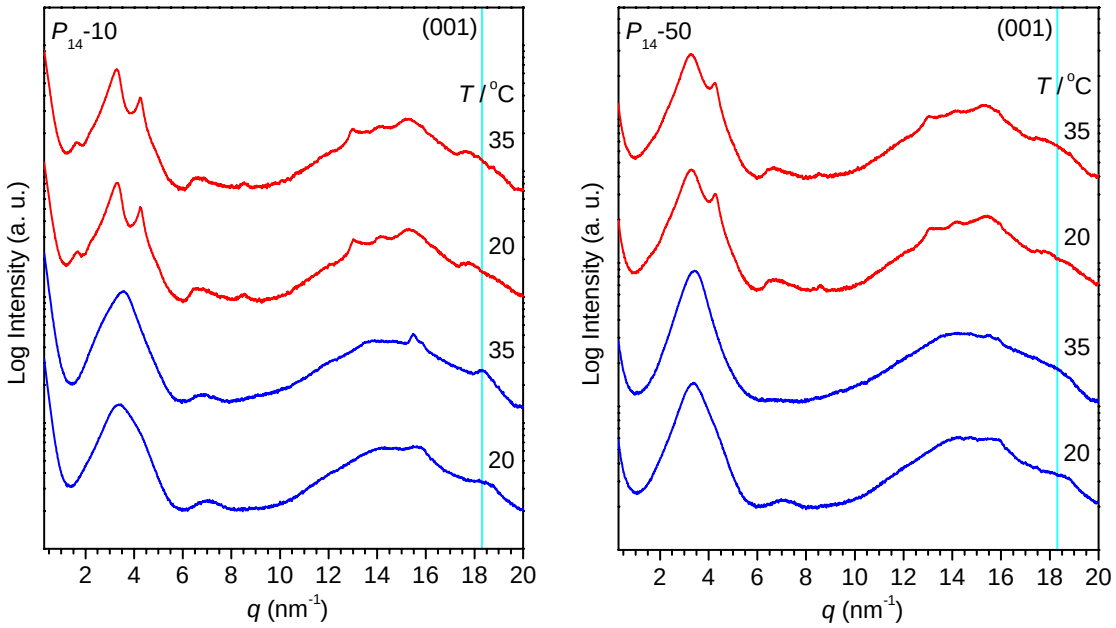

Figure S19. Variable temperature SAXS/WAXS patterns of P_{14}-*n* at indicated temperatures during the subsequent heating process after cooling from isotropic melts at a rate of 10 °C min^{-1} (blue lines) or through a stepwise cooling process (red lines).

Table S11. SAXS/WAXS data for P_9-10, P_{10}-n and P_{14}-n after a stepwise cooling process

mesophase	*hkl*	d_{obs} [Å]	d_{cacl} [Å]	lattice parameter [Å]	ρ_{calc} [a]
Col_r	200[c]	18.7	18.7	a = 37.4	1.12, 1.14 and 1.21
(20 °C)	110[c]	14.6	14.6	b = 15.9	g cm^{-3}
*C*2/*m*	310[c]	9.79	9.80	φ[b] = 47.4°	for P_9-10, P_{10}-n and
	400[c]	9.35	9.35		P_{14}-n, respectively
	220[c]	7.31	7.31		
	330[c]	4.84	4.87		
	530[c]	4.42	4.32		
	820[c]	4.05	4.03		
		4.19 (diffuse halo)			
	001	3.43			

[a] The density, ρ, was calculated as $\rho = M \cdot Z/(N_A \cdot V_{unit\ cell})$, where $V_{unit\ cell}(Col_r) = a \cdot b \cdot c$, $Z = 2$ ($c = d_{001}/\sin\varphi$ = 4.66 Å), and M is the molecular weight of the repeat unit of 955 g mol^{-1} for P_{10}-n and 1011 g mol^{-1} for P_{14}-n, respectively. [b] Tilted angle with respect to the columnar axis, φ, calculated as $\varphi = \arcsin(\sqrt{3} \cdot b/a)$. [c] This indexation is consistent with the extinction rule of a 2D rectangular *C*2/*m* lattice: (*hk*): $h + k = 2i + 1$.

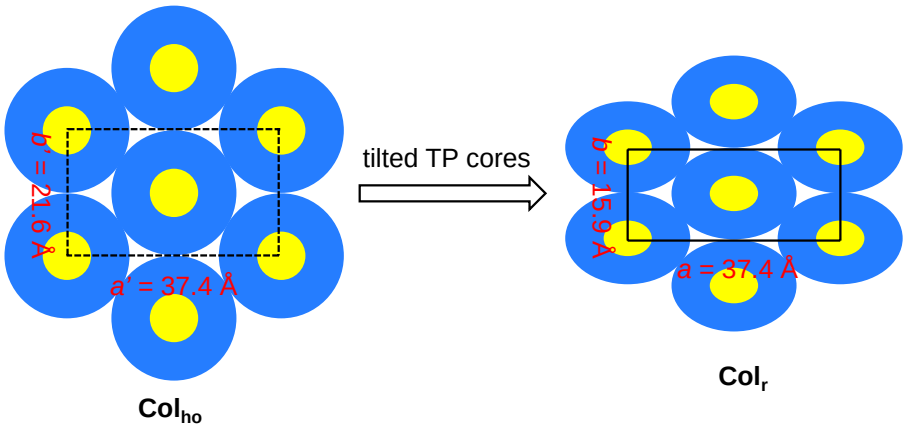

Figure S20. Proposed structure evolution of P_9-10, P_{10}-n and P_{14}-n from Col_{ho} to Col_r with tilting of discotic mesogens (top view).

5. References for Supporting Information

(1) Wu, B.; Mu, B.; Wang, S.; Duan, J. F.; Fang, J. L.; Cheng, R. S.; Chen, D. Z. *Macromolecules* **2013**, *46*, 2916-2929.

(2) Mu, B.; Wu, B.; Pan, S.; Fang, J. L.; Chen, D. Z. *Macromolecules* **2015**, *48*, 2388-2398.

(3) Tian, L.; Yang, Y.; Wysocki, L. M.; Arnold, A. C.; Hu, A.; Ravichandran, B.; Sternson, S. M.; Looger, L. L.; Lavis, L. D. *Proc. Nat. Acad. Sci. U.S.A.* **2012**, *109*, 4756-4761.

(4) Kong, X; He, Z.; Zhang, Y.; Mu, L.; Liang, C.; Chen, B.; Jing, X.; Cammidge, A. N. *Org. Lett.* **2011**, *13*, 764-767.

(5) Kong, X.; He, Z.; Gopee, H.; Cammidge, A. N. *Liq. Cryst.* **2011**, *38*, 943-955.

(6) Loscher, S.; Schobert, R. *Chem. Eur. J.* **2013**, *19*, 10619-10624.

(7) Vigderman, L.; Manna, P.; Zubarev, E. R. *Angew. Chem. Int. Ed.* **2012**, *51*, 636-641.

(8) Yu, Z. Q.; Lam, J. W. Y.; Zhao, K. Q.; Zhu, C. Z.; Yang, S.; Lin, J. S.; Li, B. S.; Liu, J. H.; Chen, E. Q.; Tang, B. Z. *Polym. Chem.* **2013**, *4*, 996-1005.

(9) Chen, X. F.; Shen, Z.; Wan, X. H.; Fan, X. H.; Chen, E. Q.; Ma, Y.; Zhou, Q. F. *Chem. Soc. Rev.* **2010**, *39*, 3072-3101.

(10) Ban, J. F.; Chen, S.; Li, C.; Wang, X. Z.; Zhang, H. L. *Polym. Chem.* **2014**, *5*, 6558 – 6568.

(11) Kumar, S. *Chemistry of Discotic Liquid Crystals: From Monomers to Polymers*; Percec, V., Ed.; CRC: Boca Raton, FL, 2011.

(12) Pal, S. K.; Setia, S.; Avinash, B. S.; Kumar, S. *Liq. Cryst.* **2013**, *40*, 1769-1816.